Design and synthesis of 4,4′-π-conjugated[2,2′]-bipyridines: a versatile class of tunable chromophores and fluorophores

Olivier Maury,[a] Jean-Paul Guégan,[a] Thierry Renouard,[a] Adam Hilton,[a] Philippe Dupau,[a] Nicolas Sandon,[a] Loïc Toupet[b] and Hubert Le Bozec*[a]

[a] *Organométalliques et Catalyse: Chimie et Electrochimie Moléculaires (CNRS UMR 6509), Institut de Chimie de Rennes, Université de Rennes 1, Campus de Beaulieu, 35042 Rennes cedex, France. E-mail: lebozec@univ-rennes1.fr; Fax: +33 2 99 28 69 39*

[b] *Groupe de la Matière Condensée et Matériaux (CNRS UMR 6626), Université de Rennes 1, Campus de Beaulieu, 35042 Rennes cedex, France*

Received (in Strasbourg, France) 10th July 2001, Accepted 3rd September 2001
First published as an Advance Article on the web

A series of 4,4′-disubstituted[2,2′]-bipyridines, featuring π-conjugated substituents such as donor- (acceptor-) substituted styryl, thienylvinyl, phenylimino and phenylazo groups, have been synthesized. X-Ray structures are provided for three ligands containing –C=C–, –C=N– and –N=N– linkers, respectively. These chromophores display good to excellent thermal stabilities with decomposition temperatures of up to 350 °C. The strong influence of the nature of the endgroups and π-linkers on the optical properties is discussed. The stepwise protonation of 4,4′-dibutylaminostyryl-[2,2′]-bipyridine and its coordination behavior to different metallizc moieties [Zn(II), Hg(II), Pd(II), Re(I), Re(VII)] have also been investigated. It is found that the absorption and emission maxima can be easily tuned by these exogenous additives over a wide range of wavelengths ($360 < \lambda_{abs} < 560$ nm; $482 < \lambda_{em} < 646$ nm).

Much attention is currently devoted to the search for new molecular materials for optoelectronics due to their potential applications in photonic[1] and/or light-emitting devices.[2] Recent recognition of the great potential of π-conjugated molecules and oligomers in light-emitting diodes has triggered the emergence of a new field of research. Furthermore, extensive efforts have recently been concentrated on the synthesis of macroscopic assemblies, such as polymers or dendrimers, featuring π-conjugated push-pull nonlinear optical (NLO) chromophores.[3] This rapid development explains the increasing efforts from research laboratories to design new chemically and thermally stable molecules presenting nonlinear optical and/or luminescent properties. It is worth pointing out that for both cases the control of the molecular geometry as well as the electronic structure—which are interconnected—is of crucial importance to optimize these physical properties.[4] For example, the transparency/efficiency trade-off of NLO-phores and the light absorption/emission properties can be tuned by rational modifications of the π-conjugated backbone.[5]

Our research group has been involved for the past ten years in the study of the NLO properties of bipyridyl metal complexes.[6] We have previously shown that ligands such as 4,4′-bis(dialkylaminostyryl)-[2,2′]-bipyridines are excellent building blocks for the construction of either dipolar compounds[7] or non-dipolar metal complexes of D_3[8] and D_{2d}[9] symmetry. In these systems the NLO response is dictated by the intense intraligand charge-transfer (ICT) transition from the donor amino group to the acceptor pyridine ring, and the role of the metal fragment is that of an inductive acceptor. Another feature that these chromophores (ligands and complexes) can offer is their optical properties.[10–12] Moreover, the wide range of 4,4′-disubstituted[2,2′]-bipyridines available makes them attractive candidates for fluorescent applications and their synthetic flexibility may allow fine-tuning of the optical (absorption and emission) properties through simple changes in the ligands or metals. This paper reports the detailed syntheses, characterization, thermal and optical properties of different 4,4′-disubstituted-[2,2′]-bipyridines featuring a series of π-conjugated moieties (Chart 1). We have focused our study on π-conjugated substituents belonging to the family of *p*-phenylenevinylene, such as *p*-donor- (or acceptor-) substituted styryl, thienylvinyl, phenylazo and phenylimino groups. We show how simple modification of either the end substituent or the π-linker enables the generation of tunable chromophores. In the last part of the paper we discuss the stepwise protonation and coordination study using different metallic fragments [Zn(II), Hg(II), Pd(II), Re(I), Re(VII)] of 4,4′-bis(dibutylaminostyryl)-[2,2′]-bipyridine, which gives rise to fluorophores that span a wide range of wavelengths in the visible spectrum.

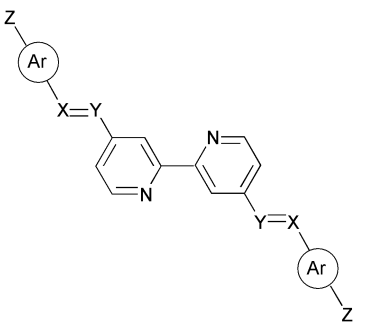

Chart 1

Results and discussion

Syntheses

Several methodologies for the preparation of the target bipyridyl ligands have been developed. Two different routes were

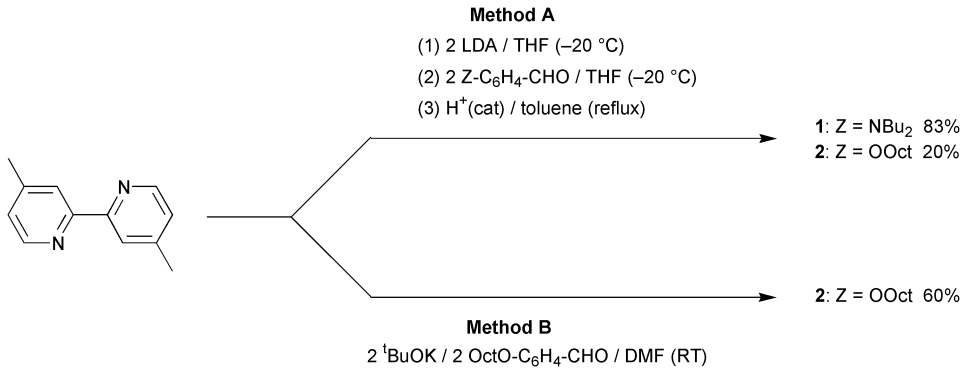

Scheme 1 Synthesis of bipyridines **1** and **2** featuring electron-donating substituents.

used for the synthesis of 4,4′-*p*-substituted styryl-[2,2′]-bipyridines **1**–**4** (Chart 2), depending on the nature of the substituent Z. The synthesis of bipyridines **1** and **2** has already been described,[13] by deprotonation of 4,4′-dimethyl-[2,2′]-bipyridine followed by addition of the corresponding aldehydes (Scheme 1, method A). Since this methodology afforded bipyridine **2** in poor yield (17%), an alternative one pot procedure was employed (Scheme 1, method B): the use of ^{t}BuOK in dimethylformamide at room temperature[14] produced **2** cleanly and in reasonable yield (60%).

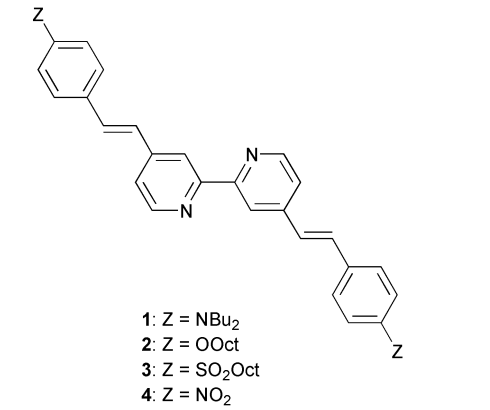

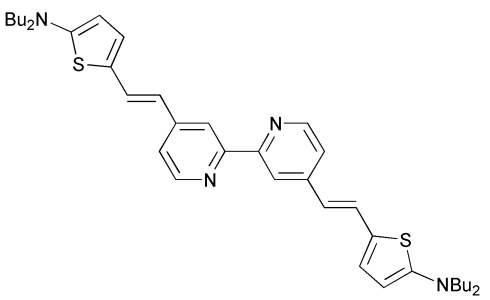

7

Chart 2

The synthesis of **3** and **4** featuring electron-withdrawing substituents (Z = –SO_2Oct, –NO_2), was achieved with 4,4′-diformyl-[2,2′]-bipyridine **5** as the building block. A new convenient two-step synthesis of the dicarboxaldehyde derivative **5** was first developed,[15] contrasting with the previous multistep procedure reported in the literature.[16] The first step involved the straightforward enamination of 4,4′-dimethyl-[2,2′]-bipyridine with the Bredereck reagent *tert*-butoxybis(dimethylamino)methane, giving rise to **6** in quantitative yield (Scheme 2). Further oxidation of the enamine groups with sodium periodate[17] in THF at room temperature furnished **5** in an overall 80% yield. A Wadworth–Emmons condensation of **5** with the appropriate phosphonates[18] gave **3** and **4** in 20 and 49% yield, respectively (Scheme 3). It is noteworthy that the presence of the long octyl chain on the sulfone moieties of **3** results in enhanced solubility as compared to the very poor solubility of **4** containing nitro acceptor end groups.

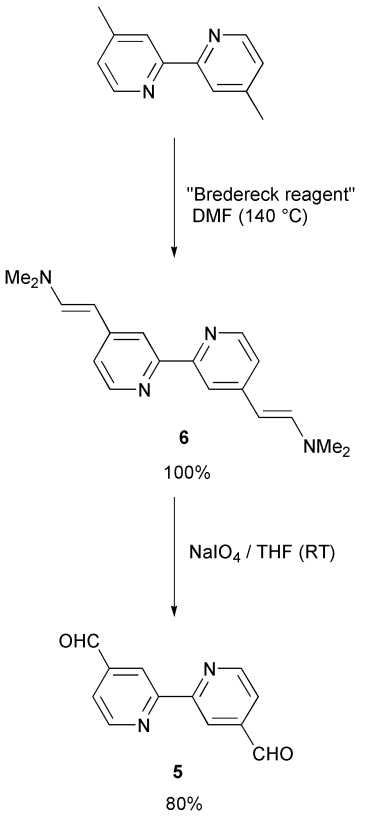

Scheme 2 Synthesis of 4,4′-diformyl-[2,2′]-bipyridine **5**.

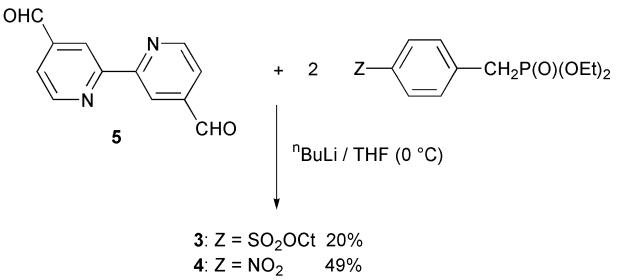

Scheme 3 Synthesis of bipyridines **3** and **4** featuring electron-withdrawing substituents.

Compound **7** (Chart 2) containing a thienyl conjugated bridge was prepared in high yield (91%) by following the synthetic sequence shown in Scheme 1 (method A) from 5-dibutylaminothiophene-2-carboxaldehyde.[19] According to the ^{1}H NMR spectrum, a mixture of *Z* and *E* isomers was formed but a slow isomerization occurred in solution and/or in the solid state to give, after several days, the thermodynamically more stable *E* isomer. The 4,4′-dialkenyl-[2,2′]-bipyridines were characterized by high resolution mass spectrometry (HRMS), as well as by ^{1}H and ^{13}C NMR (see Experimental). All the double bond linkages were confirmed to be *trans* by ^{1}H NMR analysis, based on the determination of the coupling constant $J_{CH=CH} \approx 16$ Hz.[20]

The imino-containing bipyridine **8** was synthesized in 95% yield by a Schiff base condensation reaction between *N*,*N*-diethyl-1,4-phenylenediamine and **5** in dichloromethane at room temperature[21] (Scheme 4). This compound was unambiguously characterized by the presence of strongly deshielded signals at 8.71 and 151.26 ppm, corresponding to the N(8)=C(7)H proton and carbon, respectively. In contrast to **1**–**4**, compound **8** is rather acid/moisture sensitive, and we could rapidly regenerate the starting products upon hydrolysis in the presence of traces of acid. All attempts to isolate the ''reverse'' imino-bipyridine (in this case X=Y represents a C=N double bond) from the reaction between 4,4′-diamino-[2,2′]-bipyridine and diethylaminobenzaldehyde failed, even under severe experimental conditions, confirming the already observed deactivation of the amino and carbonyl functions in the presence of acceptor and donor groups, respectively.[22] The azo-containing bipyridyl ligand **9** was synthesized by diazotation of 4,4′-diamino-[2,2′]-bipyridine **10** with sodium nitrite and subsequent coupling with *N*,*N*-dibutylaniline (Scheme 5). After chromatographic work-up, the product was isolated with a modest 25% yield as a dark red microcrystalline powder. All attempts to increase the yield, by using anhydrous conditions described in the literature for the synthesis of various diazonium salts (CF_3COOH–PenONO in CH_3CN at $-10\,^\circ$C), failed.[23] The 4,4′-diamino-[2,2′]-bipyridine precursor **10** was quantitatively prepared upon reduction of 4,4′-dinitro-[2,2′]-bipyridine-[1,1′]-dioxide[24] by hydrazine hydrate in the presence of Pd/C.[25] This mild and efficient method contrasts favorably with the known, low-yield procedure (20%) using Fe/AcOH as reducing agent.[26] Compound **9** was characterized by ^{1}H and ^{13}C NMR, and the *trans* configuration of the azo as well as the imino linkages were evidenced by an X-ray diffraction analysis (*vide supra*).

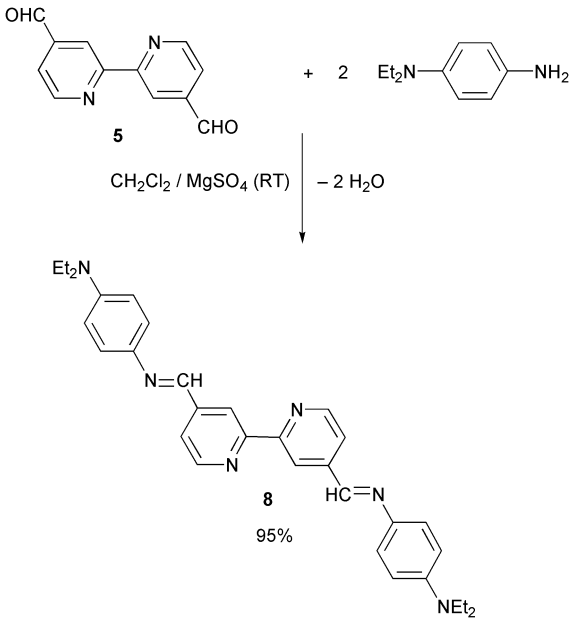

Scheme 4 Synthesis of the imino containing bipyridine **8**.

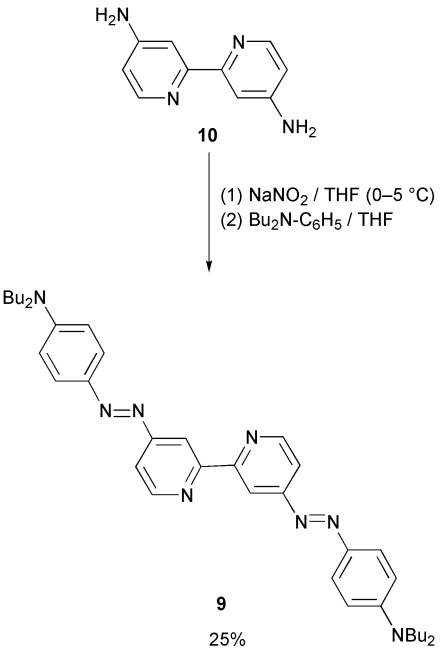

Scheme 5 Synthesis of the azo-containing bipyridine **9**.

Crystallographic structures

The structures of compounds **1**, **8** and **9** were determined by X-ray diffraction; selected bond lengths and angles, crystal data and refinement parameters are listed in Tables 1 and 2, respectively. In contrast to **8** and **9**, **1** crystallizes as a dimer in which the two molecules are roughly identical with no overlapping of the aromatic rings. In this latter case, only one molecule will be described for clarity (Fig. 1). In all cases, the bipyridines adopt the classical transoid arrangement due to the repulsion of the nitrogen lone pairs, with a symmetry center in the middle of the C2–C2′ bond for **8** and **9** (Fig. 2 and 3) and a pseudo-symmetry center for **1**.[27] The *E* configuration of the X7=Y8 double bonds and the *s-trans* conformation between the X7=Y8 and C4–C5 bonds are confirmed, whatever the nature of the X7=Y8 linkage (C=C, C=N, N=N). The planarity in the solid state can be estimated by measuring the twist angle τ between the phenyl and the pyridyl rings (Table 3). Assuming that the C4–X7–Y8–C9 atoms are coplanar, τ is the algebric sum of the dihedral angles C3–C4–X7–Y8 and X7–Y8–C9–C10. In the three structures, τ is found to be between 8.8 and 18.7°, clearly indicating the good

Table 1 Selected bond lengths and angles for **1**, **8** and **9**

Bond lengths/Å	**1** (X7 = C7, Y8 = C8)		**8** (X7 = C7, Y8 = N8)	**9** (X7 = N7, Y8 = N8)
C2–C2′	1.488 (8)		1.482 (7)	1.492 (4)
N1–C2	1.366 (13)	1.311 (12)	1.343 (4)	1.338 (3)
C2–C3	1.406 (13)	1.369 (14)	1.382 (4)	1.383 (3)
C3–C4	1.384 (15)	1.407 (15)	1.381 (5)	1.392 (3)
C4–X7	1.461 (14)	1.472 (15)	1.465 (5)	1.424 (3)
X7–Y8	1.312 (14)	1.306 (14)	1.267 (4)	1.261 (2)
Y8–C9	1.478 (14)	1.454 (15)	1.414 (4)	1.394 (3)
C9–C10	1.376 (16)	1.393 (15)	1.386 (5)	1.389 (3)
C10–C11	1.404 (15)	1.350 (14)	1.364 (5)	1.367 (3)
C11–C12	1.389 (15)	1.358 (14)	1.395 (5)	1.411 (3)
Angles/°				
C5–C4–X7	118.9 (10)	119.4 (10)	121.5 (4)	116.6 (2)
C4–X7–Y8	124.1 (11)	128.7 (10)	120.1 (4)	113.40 (19)
X7–Y8–C9	126.8 (11)	129.2 (10)	121.0 (3)	114.63 (19)

Table 2 Selected crystallographic and data collection parameters for **1**, **8** and **9**

	1	**8**	**9**
Formula	$C_{80}H_{76}N_8$	$C_{16}H_{18}N_3$	$C_{19}H_{25}N_4$
M/g	1149.49	252.33	309.43
Crystal system	Triclinic	Monoclinic	Monoclinic
Space group	$P\bar{1}$	$P2_1/c$	$P2_1/c$
a/Å	11.915 (3)	7.309 (3)	10.145 (4)
b/Å	12.050 (4)	7.698 (5)	10.820 (4)
c/Å	13.544 (2)	25.101 (7)	16.051 (9)
α/°	105.67 (2)	90	90
β/°	99.141 (10)	92.13 (2)	96.949 (5)
γ/°	93.40 (2)	90	90
U/Å^3	1837.9 (8)	1411.3 (12)	1749.0 (14)
Z	1	4	4
λ(Mo-Kα)/Å	0.71069	0.71069	0.71069
μ/cm^{-1}	0.65	0.72	0.71
T/K	293	293	293
Reflections measured	8401	3264	3813
Reflections [$I > 2\sigma(I)$]	3534	872	1802
R_1 (all data)	0.2044	0.2724	0.1568
R_1 [$I > 2\sigma(I)$]	0.0776	0.0633	0.0521
wR_2 (all data)	0.3179	0.2056	0.1732
wR_2 [$I > 2\sigma(I)$]	0.2287	0.1429	0.1378

planarity of the π-conjugated systems. Moreover, for the three compounds, the C4–X7 and Y8–C9 bond lengths fall between those of classical single and double bonds, indicating for the three structures a good delocalization along the π-conjugated backbone.

Optical properties

Influence of the substituents. 4,4′-Substituted styryl-[2,2′]-bipyridines **1**–**3** show different UV-visible spectra, depending on the nature of the substituent Z. The optical spectra of "push-pull" molecules **1** and **2** are characterized by an intense, structureless and broad absorption band at 400 and 337 nm, respectively, which can be assigned to an intraligand charge-transfer transition (ICT).[13] In contrast, bipyridine **3** featuring the electron-withdrawing group SO_2Oct can be considered as a "pull-pull" molecule, and thus exhibits maxima in the UV region at 275 and 300 nm assigned to π–π* transitions. Photoluminescence is observed for the three compounds in dichloromethane solution at room temperature, and the emission maxima are also strongly dependent on the nature of Z (Table 4 and Fig. 4). A blue emission is observed at $\lambda_{em} = 363$ nm for **3**, whereas **1** and **2** each display an emission band in the visible, that of **1** being as expected red-shifted with respect to that **2** (**1**, $\lambda_{em} = 497$ nm; **2**, $\lambda_{em} = 411$ nm).

Solvatochromic measurements were performed for compound **1** by using seven different solvents (Table 5). The correlation between the absorption and emission energies *vs.* Reichardt's E^T polarity scale[28] is presented in Fig. 5. A small positive solvatochromism (*i.e.*, bathochromism) of the absorption band is observed, which is consistent with an ICT transition. These results compare well with the optical spectra of the related 4,4′-diethylaminostyryl-[2,2′]-bipyridine[10a] and those of chromophores like bis(3,8-*p*-substituted-phenylethynyl)phenanthroline[11] or bis(6,6′-*p*-substituted-styryl)-[3,3′]-bipyridine.[12]

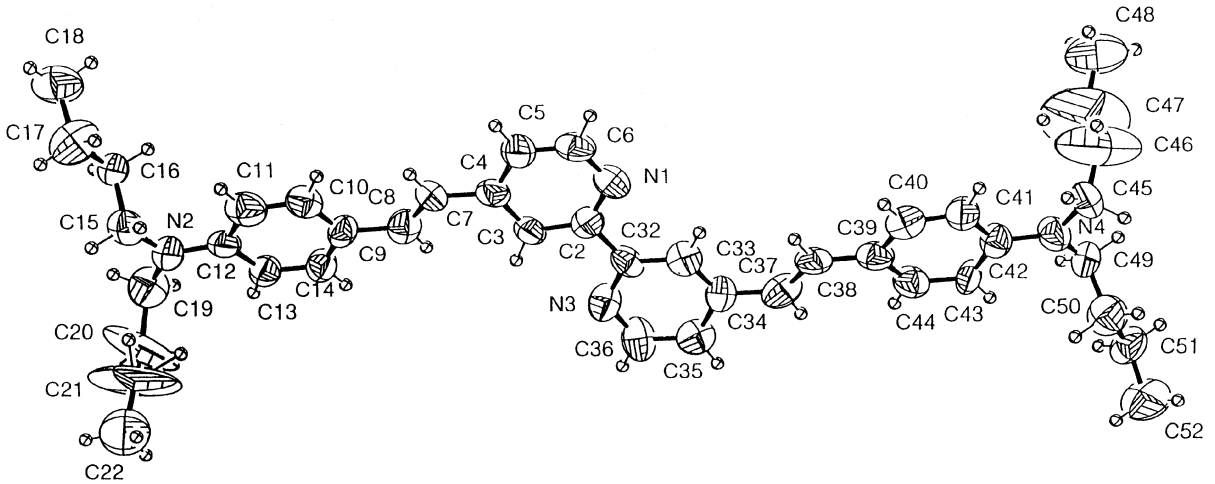

Fig. 1 ORTEP drawing of compound **1**; for clarity only one molecule is represented.

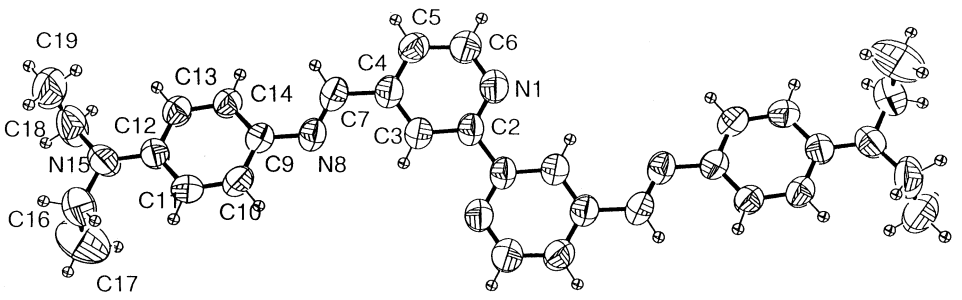

Fig. 2 ORTEP drawing of compound **8**.

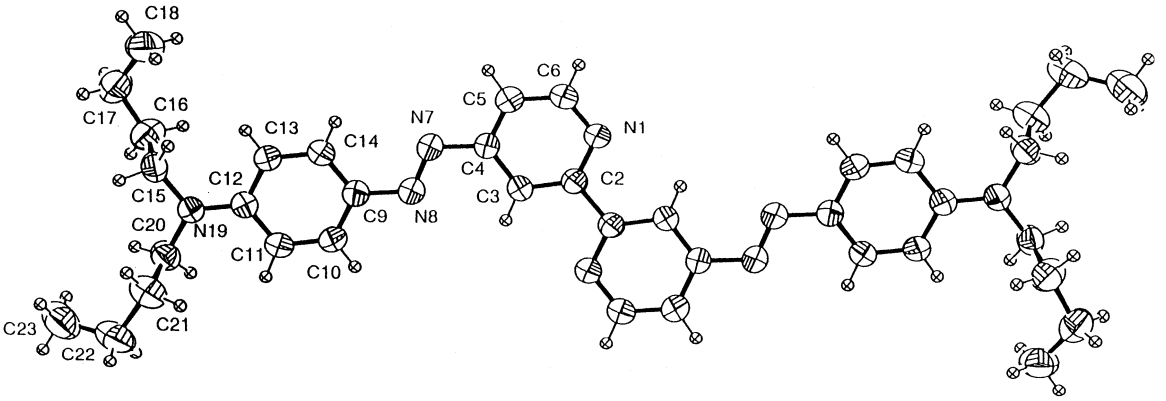

Fig. 3 ORTEP drawing of compound **9**.

Table 3 Twist angle τ between the phenyl and pyridyl rings for **1**, **8** and **9**

	Dihedral angle/°			
	C4–X7–Y8–C9	C3–C4–X7–Y8	X7–Y8–C9–C10	τ/°
1	177.0	7.3	4.2	11.5
	180.0	16.8	1.9	18.7
8	179.6	5.8	12.8	18.6
9	179.4	3.5	5.3	8.8

Table 4 Optical data of the studied compounds in dichloromethane

Ligand	λ_{max}/nm	ε/L mol^{-1} cm^{-1}	λ_{em}/nm	Stokes shift/nm	Φ_F
1	401	65000	497	96	0.23[a]
2	337	34000	411	74	0.01[b]
3	275, 300[c]	—	363	88	0.03[b]
6	345	38000	449	104	0.015[b]
7	443	69000	528	85	0.015[a]
8	433	53000	—	—	—
9	473	64000	—	—	—

[a] Relative quantum yield determined using fluorescein as standard. [b] Relative quantum yield determined using quinine sulfate as standard. [c] Not an ICT band.

Influence of the π-conjugated system. The effect of the π-linker (between the pyridyl and donor endgroups) on the optical properties has been studied by using the same donor substituent, a dialkylamino group.[29] As the π-conjugated systems can contain a X=Y double bond and an aromatic fragment that can be independently modified, two classes of chromophores were considered for comparison. The first class features a C=C double bond, which can either be directly linked to the dialkylmino group (**6**) or bonded to an aromatic ring,/phenyl (**1**) or thienyl (**7**). In the second class of chromophores, the π-conjugated bridge contains an X=Y double bond, which can be either C=C (**1**), N=C (**8**) or N=N (**9**), associated with a phenyl group. The absorption and emission data for these different chromophores are gathered in Table 4 and Fig. 6. An elongation of the conjugated bridge, as when going from **6** to **1**, induces a red shift of the ICT band ($\Delta\lambda_{max} = 58$ nm).[30] Moreover, the substitution of the phenyl ring in **1** for a thiophene ring in **7** results in a further substantial bathochromic shift by 42 nm.[31] This behavior is in accord with other studies on push-pull thiophene stilbene derivatives,[32] and can be explained by (i) the lower aromatic stabilization energy of the thienyl *vs.* the phenyl moieties (28 *vs.* 36 kcal

Table 5 Solvatochromic behavior of **1** and **7**

	1		**7**	
Solvent	λ_{max}/nm	λ_{em}/nm	λ_{max}/nm	λ_{em}/nm
Toluene	392	440	429	496
THF	393	479	432	513
Acetone	395	497	441	521
CH_2Cl_2	399	497	443	532
DMF	403	513	446	531
DMSO	408	525	451	541
EtOH	403	505	444	540

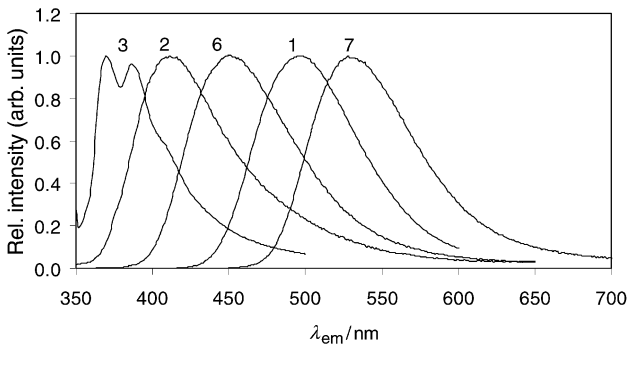

Fig. 4 Emission spectra of bipyridines **1**–**3**, **6** and **7** in dichloromethane. Intensities of the spectra have been normalized to 1.

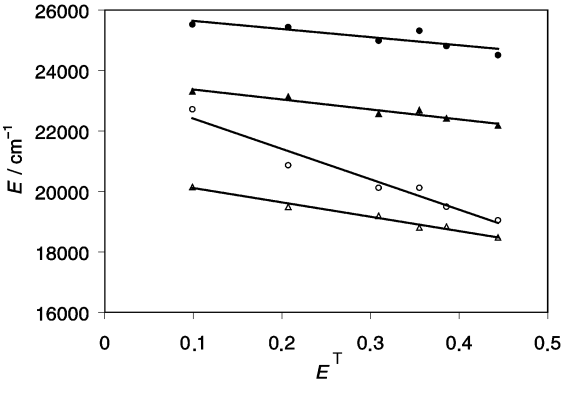

Fig. 5 Energy maxima *vs.* the Reichardt solvent parameter for **1** and **7** in absorption (filled symbols) and emission (open symbols), respectively.

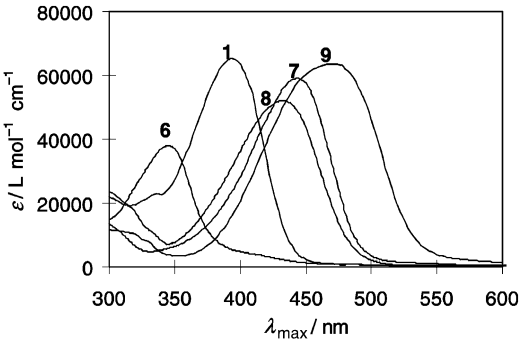

Fig. 6 Influence of the π-linker on the absorption properties.

mol^{-1}), which allows a better delocalization,[33] and (ii) its auxiliary donor property, which increases the intramolecular charge transfer.[34] These different effects can also be observed in the luminescence spectra of **6**, **1** and **7**, where the emission maxima are found at 449, 497 and 528 nm, respectively. Moreover, the nature of the linker has a dramatic influence on the quantum yield (Φ_F) of the chromophores (Table 4). For instance, a considerable drop in fluorescence quantum efficiency is observed upon replacement of the phenyl by thienyl ring ($\Phi_F = 23\%$ for **1** and 1.5% for **7**). The incorporation of nitrogen atoms into the double bond of the transmitter induces a significant shift of the ICT transition to lower energy. Thus, compound **8** (C=N) is red-shifted by 33 nm relative to **1**, and furthermore **9** (N=N) is red-shifted by 38 nm relative to **8**. Similar behavior has been observed for other organic or organometallic chromophores. For example, a bathochromic shift of 40 nm between 4-dimethylamino-4′-dimethylsulfonylazobenzene and the corresponding stilbene derivative,[18b] and a red shift of 20 nm occurred on changing from a stilbene to an iminobenzene ruthenium complex.[22] According to theoretical studies,[35] this significant bathochromic shift seems to be due to the higher electronegativity of the nitrogen, which induces a supplementary dipole moment enforcing the overall molecular charge transfer. Finally it is worth noting that, in contrast to **1**, compounds **8** and **9** do not display any emission in solution at room temperature.

Thermal stability

Chemical and thermal stability are important requirements for practical applications, in particular for the use of chromophore dopants in a polymeric or inorganic matrix. Except for **8**, the current family of chromophores is chemically inert toward air or water as the molecules were found to remain unchanged over several months in an open flask. The determination of their thermal decomposition temperatures T_{d_5} (5% loss of weight) and $T_{d_{10}}$ (10% loss of weight) was investigated by thermogravimetric analysis (TGA) under nitrogen (Table 6).

Table 6 Melting points and thermal stabilities of compounds **1**–**3** and **6**–**9**

Ligand	Mp/°C	T_{d_5}/°C	$T_{d_{10}}$/°C
1	147	355	380
2	146	350	370
3	—	195	260
6	185	205	230
7	144	275	310
8	Decomp.	—	—
9	138	205	250

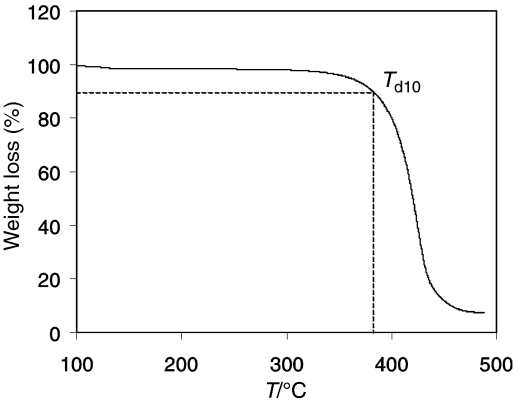

Fig. 7 Thermogravimetric analysis of **1**.

As an example, the TGA of compound **1** is reported in Fig. 7: no loss of weight occurs up to 350 °C and the thermal decomposition temperatures T_{d_5} and $T_{d_{10}}$ are found at 355 and 380 °C, respectively. It should be noted that the UV-visible and ^{1}H NMR spectra of **1** remain unchanged after 60 min exposure at 310 °C under nitrogen, confirming the high thermal stability of this chromophore. The T_d values depend strongly on the nature of the π-conjugated groups. Thermal decomposition of the styryl bipyridine compounds **1**–**3** does not occur below 260 °C, the more stable being the push-pull chromophores **1** and **2** ($T_{d_5} \approx 350$ °C). However, the introduction of a thienyl ring in place of a phenyl leads to a decrease of the T_{d_5} value (275 °C).[32c] Moreover, compound **9** bearing an azo bridge has a relatively low decomposition temperature ($T_{d_5} = 205$ °C), whereas for **8**, decomposition occurs prior to melting. Thus, the styryl bipyridine derivatives appear to be the most thermally robust chromophores, comparable to the highest thermal stability reported in the literature,[36] which makes them good candidates for incorporation into a host matrix.

Modulation of the optical properties

Stepwise protonation of 1 with *p*-toluenesulfonic acid. As the 4,4′-bis(dibutylaminostyryl)-[2,2′]-bipyridine **1** contains four potentially basic sites—the imino groups of the two pyridyl rings and the amino functions of the two dialkylamino substituents—a stepwise protonation was carried out by using *p*-toluenesulfonic acid (PTSA). The reaction was followed by UV-visible and emission spectroscopy (Fig. 8 and Table 7). The addition of one equivalent of PTSA to a dichloromethane solution of **1** promotes a rapid color change, from yellow to deep red. The UV-visible spectrum shows a one-half decrease in

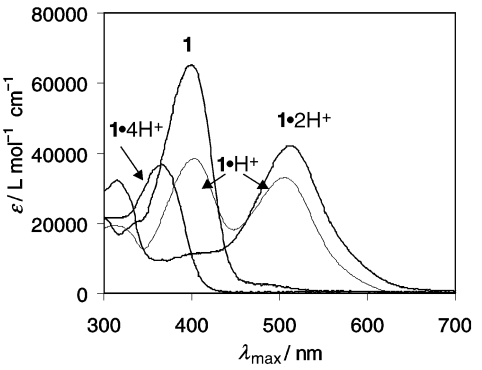

Fig. 8 UV-visible spectra of **1** and **1**·xH$^+$ ($x = 1$, 2 and 4) in dichloromethane.

Table 7 Optical data for compounds **1** and **1**·xH$^+$ in dichloromethane

PTSA (equiv.)	λ_{max}/nm ($\varepsilon \times 10^{-3}$/L mol^{-1} cm^{-1})			λ_{em}/nm		
0		400 (65)			497	
1	311 (16)	400 (38)	510 (33)		497	632
2	311 (32)		510 (42)			632
4	360 (37)			482		

the intensity of the charge transfer band at 400 nm band and the appearance of two new absorption bands at 510 and 311 nm, which can be assigned to ICT and π–π* transitions, respectively.[37] The presence of two CT bands in the visible region suggests that the protonation occurs only on one pyridinic site of **1**, giving rise to **1**·H$^+$ (Scheme 6). The addition of a second equivalent of PTSA causes the disappearance of the band at 400 nm whereas the two intense transitions at 510 and 311 nm are still observed, as expected by the selective formation of the bipyridinium salt **1**·2H$^+$. The large bathochromic shift ($\Delta\lambda = 110$ nm) is consistent with the strong electron-accepting nature of the pyridinium ring compared with pyridine. This behavior can be compared with that of the aminostilbazole series, which exhibits a red shift of *ca.* 110 nm after methylation of the pyridinic site.[30c,38] Similarly, a bathochromic shift of the emission ($\Delta\lambda_{em} = 135$ nm) is observed, yielding a red fluorescence at 632 nm for **1**·2H$^+$. The addition of two further equivalents of PTSA to **1**·2H$^+$ produces a dramatic color change of the solution, from deep red to colorless, and the corresponding absorption spectrum displays only one maximum at 360 nm (Fig. 8). A profound blue shift of the emission is also observed: excitation at 360 nm results in one weak emission at 482 nm. Such a blue shift is consistent with the production of **1**·4H$^+$ in which the protonation of the two dialkylamino donor end groups inhibits charge transfer and raises the energy of the transition.[39] All these protonation reactions are reversible and addition of an aqueous solution of $NaHCO_3$ reforms the starting bipyridine **1**. Thus, it appears that the absorption and emission properties of a given chromophore can be tuned over a large range ($360 < \lambda_{max} < 510$ nm; $482 < \lambda_{em} < 632$ nm) simply by adding a controlled amount of acid.

Formation of a 1 : 1 adduct between 1 and tetrachlorocatechol. Crystal engineering of 1 : 1 or 1 : 2 adducts between substituted pyridines and phenol derivatives has been efficiently used in nonlinear optics to enhance the hyperpolarizability β of the neutral molecules by acid–base proton transfer.[40] Depending on the values of the ΔpK_a between the acid and the base, two types of interactions can be observed, either adducts linked by O–H···N hydrogen bonds or ionic adducts linked by N$^+$–H···O$^-$ interactions.[41] Both situations have already been described in the literature depending on the nature of the substituents on the pyridine or phenol derivatives.[42] With the goal of understanding how such types of adducts can modulate the optical properties of our chromophores, we have selected as a model system the interaction between **1** and a 1,2-benzenediol derivative, tetrachlorocatechol. Addition of one equivalent of this diol to a dichloromethane solution of **1** promotes an instantaneous color change, from yellow to yellow–brown. In the NMR spectrum, the phenol protons show a strong low-field shift with respect to those of the free catechol ($\Delta\delta \approx 2$). The aromatic region gives rise to signals that are diagnostic of a symmetric 1:1 adduct (Scheme 7): a shielding of *ca.* 0.2 and 0.4 ppm is observed for the H6 and H3 protons, respectively, in accordance with a conformational transoid–cisoid change of **1** upon interaction with the 1,2-diol. In the UV-visible spectrum, the charge transfer band is red-shifted by 13 nm ($\lambda_{max} = 414$ nm) relative to **1**.[43] This small bathochromic shift, as compared to **1**·2H$^+$ ($\Delta\lambda = 110$ nm), suggests that the

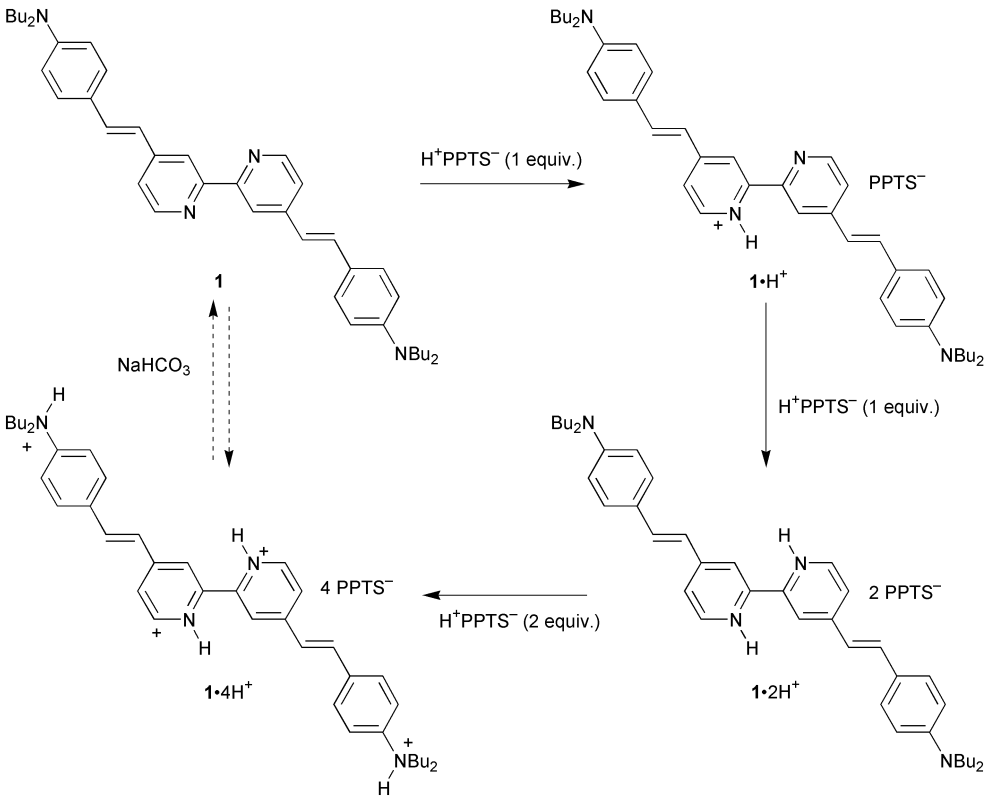

Scheme 6 Stepwise protonation of **1**.

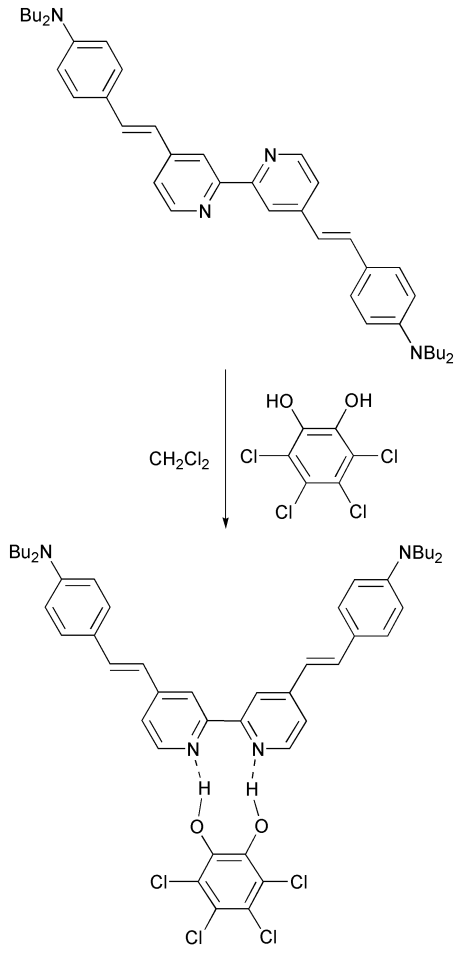

Scheme 7 Formation of a 1 : 1 adduct between **1** and tetrachlorocatechol.

interaction can be best described by the formation of a neutral adduct in which two O–H···N hydrogen bonds are formed.

Modulation of the electronic properties by complexation. Bipyridyl metal complexes represent an important class of chromophores as they offer a large range of metals with different oxidation states and ligands that can give rise to tunable optical properties. For the design of new dipolar chromophores for nonlinear optics, we have recently developed the synthesis of push-pull complexes containing bipyridyl ligands and acceptor organometallic fragments such as MX_2 (M = Zn, Hg) and $Re(CO)_3X$.[7b] The results obtained with such systems revealed an enhancement of the molecular hyperpolarizabilities and a bathochromic shift of the charge transfer band, which were sensitive to the Lewis acidity of the organometallic fragment. The goal of the present study is to explore how the optical properties of bipyridyl ligands such as **1** can be tuned by varying the metal and its oxidation state.

The Hg(II), Zn(II) and Pd(II) complexes **1a**–**d** (Chart 3) were readily prepared upon room temperature treatment of **1** with $HgCl_2$, $ZnCl_2$ $ZnOAc_2$, and $PdCl_2$, respectively. The rhenium(I) complex **1e** was classically obtained from $Re(CO)_5Cl$ and **1** in refluxing toluene,[7b,10a] whereas the violet rhenium(VII) compound **1f** was synthesized by reacting **1** with Re_2O_7 (0.5 equiv.) in dichloromethane at room temperature. All these complexes were fully characterized by means of ^1H and ^{13}C NMR, UV-visible and fluorescence spectroscopy (Table 8) and gave satisfactory microanalyses (see Experimental). The *E* configuration of the double bond is clearly established on the basis of the strong olefinic proton coupling constant ($^3J_{H7-H8} \approx 16$ Hz) for **1a–f**, showing that there is no isomerization of the C=C linker upon complexation.[44] It should be noted that these complexes adopt different geometries such as tetrahedral for the Hg(II) and Zn(II) in **1a–c**, square planar for the Pd(II) in **1d** and *fac*-octahedral for the Re(I) complex **1e**.[7b,10a] The symmetric structure of the Re(VII) dimer **1f** is reflected in its ^1H and ^{13}C NMR spectra, which exhibit the pattern of three C–H signals for the aromatic region of the bipyridyl moieties. Moreover, the IR spectrum reveals the presence of a strong $\nu_{Re=O}$ vibration at 911 cm^{-1} and a weaker one at 967 cm^{-1}, as usually observed for related RO–ReO_3 complexes (R = K, $SnMe_3$).[45] From these spectroscopic data, we can assume that both metallic centers are equivalent in **1f** and adopt a facial octahedral geometry (Chart 3). A similar geometry has already been described for a Mo(VI) dioxo-μ-oxo dimer featuring a 4,4′-di-*tert*-butyl-[2,2′]-bipyridine ligand.[46] The thermal stability of complexes **1a–f** was determined by thermogravimetric analysis and the TGA data are collected in Table 8. It is noteworthy that, except for the Hg(II) and Re(VII) derivatives, these complexes display high thermal stability comparable to that of the ligand precursor **1**.

The complexation induces a substantial bathochromic shift of the absorption bands, which is sensitive to the nature of the metallic moiety (Table 8). For instance, in the case of **1b**, a red shift of *ca*. 60 nm in the absorption maximum is observed. For a given (**1**)MCl_2 structure, this red shift can be tuned by the Lewis acidity of the metal ion and, as expected, Hg(II) complex **1a** has a smaller shift in absorption ($\Delta\lambda_{ICT} = 37$ nm) than Zn(II)-containing **1b** ($\Delta\lambda_{ICT} = 58$ nm). However, whereas Pd(II) is a weaker Lewis acid than Zn(II),[47] a more pronounced red shift is observed for **1d** ($\Delta\lambda_{ICT} = 80$ nm). Thus, it appears that other factors such as the geometry of the complexes can play a non-negligible role: in contrast to the Zn(II) and Hg(II) complexes, which adopt a tetrahedral geometry, the d^8-Pd(II) complex is square planar and thus, the two chloride ligands lie *trans* to the pyridyl rings. The influence of the ancillary ligands as well as of the oxidation state on the optical properties is clearly shown by comparing the optical spectra of the two Re(I) and Re(VII) complexes **1e** and **1f**; the absorption maximum shifts from 473 nm for **1e** to 559 nm for **1f**. Photoluminescence is also observed for all the complexes in dichloromethane solution (Table 8). A substantial red shift of the emission band, from 120 to 150 nm, is found when compared to that of the free ligand **1**. However, it should be noted that the modulation of the emission wavelength upon varying the metallic moiety occurs in a more narrow range ($\Delta\lambda_{em} \approx 35$ nm) than for the absorption band ($\Delta\lambda_{abs} \approx 120$ nm). Finally, complexation of **1** can also influence profoundly the fluorescence quantum yield. For example, whereas the Hg(II) derivative **1a** emits with a fluorescence intensity similar to that of the ligand ($\Phi_F = 21\%$), the quantum yields for the Zn(II) complexes **1b–c** are more than threefold enhanced ($\Phi_F \approx 70\%$) (Fig. 9). Such a chelation-enhanced fluorescence much precedent with the Zn(II) ion,[48] and the use of polydentate ligands like substituted sulfonamidoquinolines, dipicolylamines, and macrocyclic tetraamines has recently been reported to give efficient zinc(II) fluorophores for biological applications.[49]

Conclusions

In this study we have described the syntheses, thermal stabilities and optical spectra for a versatile family of 4,4′-π-conjugated[2,2′]-bipyridines. Tuning of the electronic absorption properties is made possible by simple modification of the endgroup and π-linker. For the 4,4′-*p*-substituted styryl-[2,2′]-bipyridine series, the bathochromic shift is consistent with relative values of the donor strengths in the order $NBu_2 > OOct > SO_2Oct$. With a given donor group such dialkylamino, a substantial red shift of the ICT

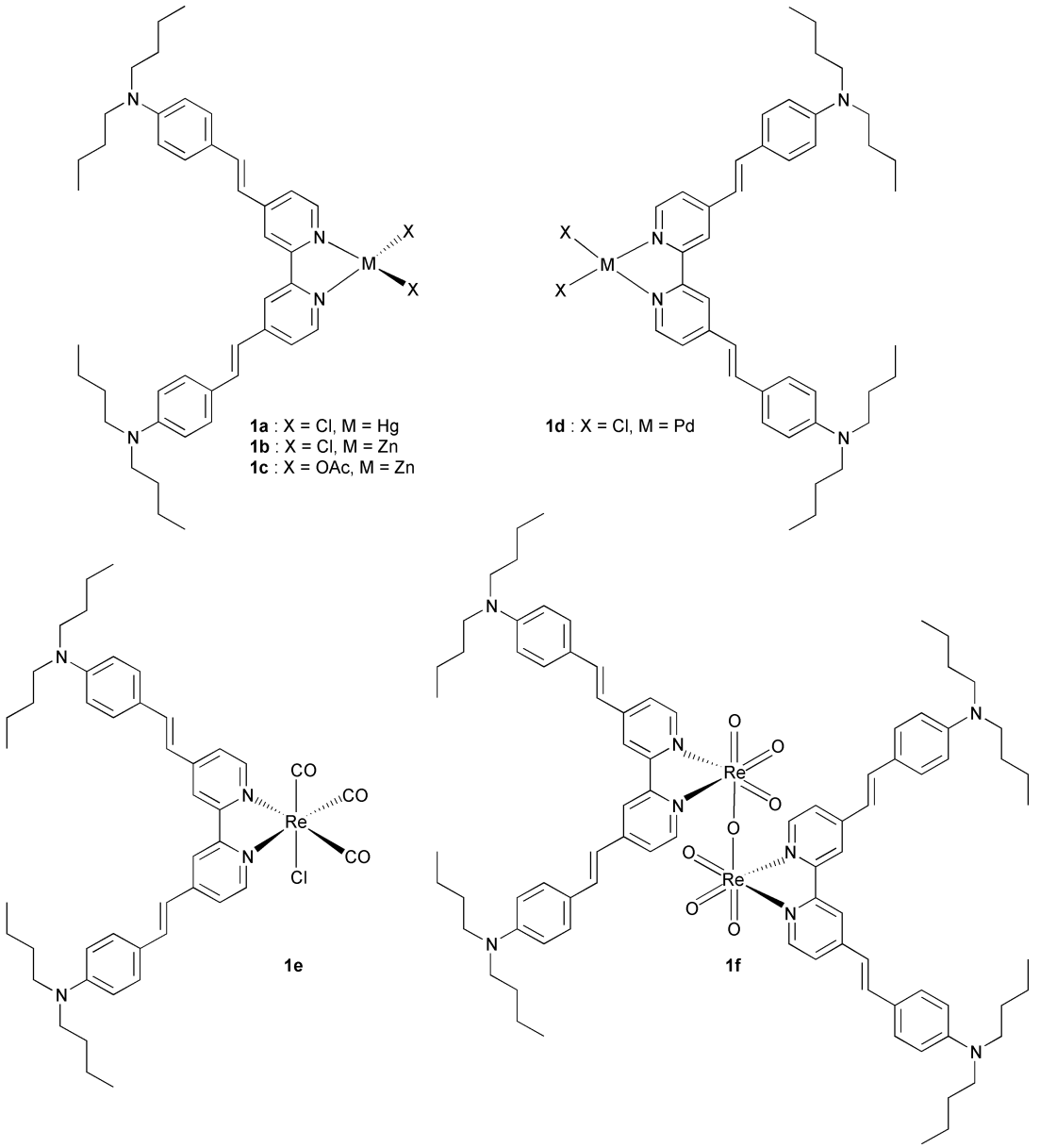

Chart 3

Table 8 Optical data (in dichloromethane) and thermal stabilities of complexes **1a**–**1f**

Complex		λ_{max}/nm	ε/L mol^{-1} cm^{-1}	λ_{em}/nm	Stokes shift/nm	Φ_F	T_d–$T_{d_{10}}$/°C
(**1**)$HgCl_2$	**1a**	438	51000	615	177	0.21	192–206
(**1**)$ZnCl_2$	**1b**	459	62000	624	164	0.74	392–399
(**1**)$Zn(OAc)_2$	**1c**	444	60000	610	166	0.65	353–367
(**1**)$PdCl_2$	**1d**	481–383	63000–26000	622	141	—	312–321
(**1**)$ReCl(CO)_3$	**1e**	473–381	67000–30000	630	157	—	382–392
[(**1**)ReO_3]$_2$-μ^2-O	**1f**	559	80000	646	87	—	228–360

transition occurs in the following order: phenylazo > thienylvinyl > phenylimino > styryl > vinyl. The emission energy and fluorescence efficiency are also dictated by the nature of the end substituents and π-conjugated systems: substitution of a phenyl by a thienyl ring results in a red shift in emission wavelength and substantial decrease in fluorescence quantum yield, whereas introduction of nitrogen atoms in the π-linker produces an extinction of the fluorescence. Finally, the optical properties of a given chromophore show a fine degree of tunability upon either stepwise protonation or metal coordination. Notably, depending on the controlled amount of protons but also on the Lewis acidity of the metallic fragment and/or the geometry of the resulting complex, further modulation can be achieved over a large range of absorption and emission wavelengths ($360 < \lambda_{abs} < 560$ nm; $482 < \lambda_{em} < 646$ nm).

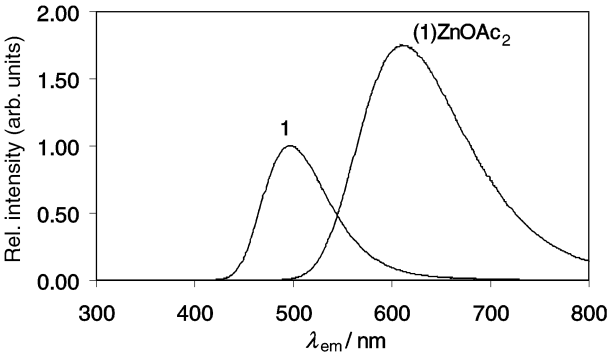

Fig. 9 Comparison of the emission spectra of **1** and **1b** in dichloromethane at the same concentration.

Experimental

General procedures

All reactions were routinely performed under argon using Schlenk techniques. NMR spectra (^{1}H, ^{13}C, ^{31}P) were recorded at room temperature on a Bruker DPX 200 (operating at 200.12 MHz for ^{1}H) or on a Bruker AC 300 (operating at 300.13 MHz for ^{1}H) spectrometer. NMR data are listed in parts per million (ppm) and are reported relative to tetramethylsilane (^{1}H, ^{13}C), residual solvent peaks being used as internal standard (CD_2Cl_2 ^{1}H: 5.25 ppm; ^{13}C: 53.45 ppm). Complete assignment of the ^{1}H and ^{13}C spectra required 2D experiments [COSY, H–C correlation (HMQC and HMBC sequences)]. The atom numbering for bipyridyl ligands and related complexes is depicted Fig. 10.

UV-visible spectra were recorded on a Kontron UVIKON 941 spectrophotometer in dilute dichloromethane solution (*ca.* 10^{-5} mol L^{-1}). Infra-red spectra were recorded in KBr pellets using a Nicolet 205 FTIR. Thermal stability was measured by means of a TA Instrument TGA 2050 thermogravimetric analyzer, decomposition temperature at 5 and 10% weight lost are called T_{d_5} and $T_{d_{10}}$ respectively, and below are reported quoted to the 5 °C inferior. The heating program used was the following (i) isothermal at 50 °C for 15 min, (ii) a temperature ramp of 10 °C min^{-1} up to 600 °C. Melting points were measured using a TA Instrument DSC 2010 differential scanning calorimeter. High resolution mass spectrometry measurements (FAB or EI) were performed at the Centre Regional de Mesures Physiques de l'Ouest (Rennes, France) and elemental analysis by the Service Central d'Analyse du CNRS (Solaize, France).

Fluorescence analysis

Fluorescence experiments were performed in dilute dichloromethane solution (*ca.* 10^{-5}–10^{-6} mol L^{-1}) using a PTI spectrometer. Fluorescence quantum yields were measured on non-degassed samples at room temperature. Solutions of fluorescein in NaOH (1 M) or of quinine sulfate in H_2SO_4 (1 M) were used as standards for the quantum yield measurement ($\Phi_F = 0.90$ and $\Phi_F = 0.546$, respectively). Refractive index corrections have been performed.[50]

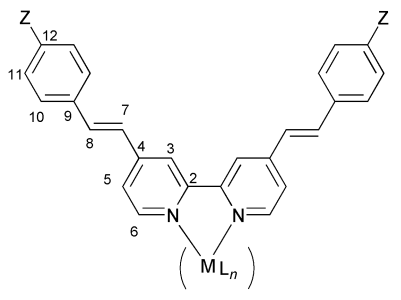

Fig. 10 Generic atom numbering of the *p*-substituted styryl-[2.2′]-bipyridyl ligands and related complexes. The labels are used for the assignment of the ^{1}H and ^{13}C NMR signals.

Crystal structure analysis

The samples were studied on an CAD4 NONIUS automatic diffractometer with graphite monochromated Mo-Kα radiation.[51] The cell parameters were obtained by fitting a set of 25 high-theta reflections. After Lorentz and polarization corrections,[52] the structure was solved with SIR-97,[53] which revealed the non-hydrogen atoms of the structure. After anisotropic refinement all the hydrogen atoms were found with a Fourier difference synthesis. The whole structure was refined with SHELXL97[54] by the full-matrix least-squares techniques [use of *F* magnitude; *x*, *y*, *z*, (*ij* for C, N and O atoms, *x*, *y*, *z* in riding mode for H atoms)]. ORTEP views were realized with PLATON98.[55] All the calculations were performed on a Silicon Graphics Indy computer.

CCDC reference numbers 166922–166924. See http://www.rsc.org/suppdata/nj/b1/b106096c/ for crystallographic data in CIF or other electronic format.

Chemicals

p-Dibutylaminobenzaldehyde was synthesized on the 15 g scale, in a one-step reaction using the classical Vilsmeier–Haack formylation. 5-Dibutylaminothiophene-2-carbaldehyde[19] was synthesized in 70% yield using dimethylsulfoxide as solvent instead of water and the purification of the crude product was carried out by distillation under reduced pressure (125 °C under 0.05 mm Hg). The synthesis of 1-methyl-4-(octane-1-sulfonyl)benzene,[56] and 4-octyloxybenzaldehyde[57] were carried out using published methods. 4,4′-Dinitro-[2,2′]-bipyridine-[1,1′]-dioxyde was classically synthesized.[24] (***Caution***! During this nitration reaction a violent explosion occurred.) *N*,*N*-Diethyl-1,4-phenylenediamine (ACROS) was distilled just before used under reduced pressure. $NaIO_4$ was purchased from Aldrich in a 5 g bottle.[58] Tetrachloro-1,2-benzenediol was purchased from Lancaster and purified by recrystallization from hot toluene. THF was distilled over Na–benzophenone, DMF was distilled prior to use, toluene was distilled over Na and CH_2Cl_2 was distilled over P_2O_5.

Syntheses

4,4′-Bis(dibutylaminostyryl)-[2,2′]-bipyridine (1). The bipyridyl ligand 4,4′-bis(dibutylaminostyryl)-[2,2′]-bipyridine was synthesized using a previously reported procedure.[13b] Single crystals suitable for X-ray diffraction analysis were obtained by slow diffusion of pentane in a dichloromethane solution. ^{13}C NMR (CD_2Cl_2): δ 156.08 (C2), 148.31 (C12), 146.22 (C4), 148.90 (C6), 133.02 (C8), 128.14 (C10), 122.79 (C9), 120.16 (C7), 119.84 (C5), 117.10 (C3), 111.14 (C11), 50.33 (C13), 29.08 (C14), 19.97 (C15), 13.47 (C16).

4,4′-Bis(*p*-octyloxystyryl)-[2,2′]-bipyridine (2). In a Schlenk flask, 4,4′-dimethyl-[2,2′]-bipyridine (1 g, 5.42 mmol) and 4-octyloxybenzaldehyde (2.53 g, 10.84 mmol, 2 equiv.) were dissolved in dimethylformamide (5 mL) and ^{t}BuOK (1.51 g, 13.55 mmol) was slowly added at room temperature. The solution, which immediately turned brown, was then stirred for 2 h. Addition of water led to the formation of a pale precipitate, which was filtered off by centrifugation (15 min, 14000 pm). The crude solid was dissolved in dichloromethane, washed with water, dried over $MgSO_4$, and the solvent was removed under vacuum. Recrystallization from a

dichloromethane–pentane mixture gave **2** as a white microcrystalline powder (2 g, 60%). ^{13}C NMR (CD_2Cl_2): δ 160.28 (C4), 159.90 (C2), 149.88 (C6), 146.41 (C12), 133.16 (C8), 129.25 (C9), 128.82 (C10), 124.22 (C7), 121.08 (C5), 118.22 (C3), 115.20 (C11), 68.61 (C13), 32.28 (C14), 29.81 (C15), 29.70 (C16, C17), 26.46 (C18), 23.12 (C19), 14.32 (C20).

1-(Bromomethyl)-4-(octane-1-sulfonyl)benzene. A solution containing 1-methyl-4-(octane-1-sulfonyl)benzene (2 g, 7.4 mmol), *N*-bromosuccinimide (1.5 g, 8.4 mmol) and azoisobutyronitrile (0.1 g, 0.6 mmol) in tetrachloromethane was heated at 76 °C for 17 h. After cooling to room temperature, the solvent was removed under vacuum. The residue was dissolved in dichloromethane, washed with water and dried over $MgSO_4$. The solvent was removed and the resulting oil was purified by column chromatography (silica gel, CH_2Cl_2–pentane 1:1) to give the title product as a brown oil (2.3 g, 90%). ^{1}H NMR ($CDCl_3$): δ 7.85 (d, $J = 7.8$ Hz, 2H, –C_6H_4–), 7.55 (d, $J = 7.8$ Hz, 2H, –C_6H_4–), 4.48 (s, 2H, –CH_2Br), 3.03 (t, $J = 7.9$ Hz, 2H, SO_2CH_2), 1.66 (m, 2H, $SO_2CH_2CH_2$), 1.2 [m, 10H, –$(CH_2)_5$–], 0.83 (t, $J = 5.8$ Hz, –CH_2CH_3).

1-[(Diethylphosphonate)methyl]-4-(octane-1-sulfonyl)-benzene. Triethylphosphite (1 mL) was added dropwise to 1-(bromomethyl)-4-(octane-1-sulfonyl)benzene (1.84 g, 5.3 mmol) at 0 °C. After heating under reflux overnight, the excess triethylphosphite was evaporated and the crude brown oil was purified by column chromatography (silica gel, heptane–ether–dichloromethane 55:40:5). The title product was recovered as a colorless oil (1.3 g, 62%). ^{1}H NMR ($CDCl_3$): δ 7.81 (d, $J = 7.8$ Hz, 2H, –C_6H_4–), 7.46 (d, $J = 7.8$ Hz, 2H, –C_6H_4–), 4.11–3.94 (m, 4H, O–CH_2), 3.19 (d, $J_{H-P} = 22.4$ Hz, 2H, PCH_2), 3.03 (t, $J = 7.9$ Hz, 2H, SCH_2), 1.66 (m, 2H, SCH_2CH_2), 1.23 (t, $J = 7.0$ Hz, OCH_2CH_2), 1.2 [m, 10H, –$(CH_2)_5$–], 0.83 (t, $J = 5.8$ Hz, –CH_2CH_3). ^{13}C NMR ($CDCl_3$): δ 138.4 (d, $J_{P-C} = 8.8$ Hz, C_{ipso} or C_{para}), 137.7 (d, $J_{P-C} = 3.6$ Hz, C_{ipso} or C_{para}), 130.6 (d, $J_{P-C} = 6.5$ Hz, C_{ortho} or C_{meta}, 128.2 (d, $J_{P-C} = 2.5$ Hz, C_{ortho} or C_{meta}), 62.3 (d, $J_{P-C} = 6.8$ Hz, OCH_2CH_3), 16.3 (d, $J_{P-C} = 6.0$ Hz, OCH_2CH_3), 33.8 [d, $J_{P-C} = 137.4$ Hz, $PhCH_2P(O)(OEt)_2$), 56.3, 31.6, 28.9, 28.8, 28.2, 22.6, 22.5, 14.0 (s, OOCt). ^{31}P NMR ($CDCl_3$) δ 24.8. HRMS (EI): calc. for $C_{19}H_{33}O_5PS$ 404.1786; found 404.1798.

4,4′-Bis(*p*-octylsulfonylstyryl)-[2,2′]-bipyridine (3). In a Schlenk flask, 1-[(diethylphosphonate)methyl]-4-(octane-1-sulfonyl)benzene (1.13 g, 2.8 mmol) was dissolved in THF (50 mL) and cooled to 0 °C. ^{n}BuLi (1.6 M in hexane, 2 mL, 3 mmol) was added dropwise by means of a syringe and the solution was stirred for 1 h at room temperature. A THF solution (50 mL) of **5** (0.3 g, 1.4 mmol) was then slowly added and the mixture was heated for 3 h under reflux. After cooling to room temperature, the solution was hydrolyzed upon addition of water (40 mL). The organic phases were dried over $MgSO_4$, filtered, and the solvent was removed under vacuum. After recrystallization from ethanol, compound **3** was obtained as an orange microcrystalline powder (0.2 g, 20% yield). ^{1}H NMR (CD_2Cl_2): δ 8.65 (d, $J = 5$ Hz, 2H, H6), 8.60 (br s 2H, H3), 7.86 (d, $J = 8.5$ Hz, 4H, H11), 7.73 (d, $J = 8.5$ Hz, 4H, H10), 7.49 (d, $J = 16$ Hz, 2H, H8), 7.43 (dd, $^3J = 5$ Hz, $^4J = 1.5$ Hz, 2H, H5), 7.28 (d, $J = 16$ Hz, 2H, H7), 3.06 (br t, 8H, H13), 1.61 (m, 8H, H14), 1.20 (m, 20H, H15–19), 0.81 (br t, 12H, H20). ^{13}C NMR (CD_2Cl_2) : δ 156.17 (C2), 149.50 (C6), 144.57 (C4), 141.29 (C9), 138.50 (C12), 131.00 (C8), 129.66 (C7), 128.40 (C11), 127.35 (C10), 121.15 (C5), 118.14 (C3), 56.06 (C13), 31.46 (C14), 28.73 (C15), 28.70 (C16) 28.02 (C17), 22.51 (C18), 22.37 (C19), 23.62 (C20). HRMS (FAB): calc. for $C_{42}H_{53}N_2O_4S_2$ $[M + H]^+$ 713.3447; found 713.3430.

4,4′-Bis(*p*-nitrostyryl)-[2,2′]-bipyridine (4). In a Schlenk flask, 4-nitrobenzyl-diethylphosphonate (0.6 g, 2 mmol) was dissolved in THF (50 mL) and cooled to 0 °C. ^{n}BuLi (1.6 M in hexane, 1.3 mL, 2.1 mmol) was added dropwise by means of a syringe and the solution was stirred for 1 h at room temperature. A THF solution (50 mL) of **5** (0.21 g, 1 mmol) was then slowly added and the mixture was heated under reflux for 3 h. After cooling to room temperature, the solution was hydrolyzed upon addition of water (40 mL). The orange precipitate was filtered off, washed several times with diethyl ether and dried *in vacuo*. Compound **4** was obtained as an orange microcrystalline powder (0.22 g, 49% yield). ^{1}H NMR (DMSO-d^6): δ 8.75 (d, 2H, $J = 5.0$ Hz, H6); 8.64 (s, 2H, H3); 8.28 (d, 4H, $J = 8.4$ Hz, H11); 8.00 (d, 4H, $J = 8.4$ Hz, H10); 7.81 (d, 2H, $J = 16.2$ Hz, H8); 7.75 (d, 2H, $J = 5.0$ Hz, H5); 7.70 (d, 2H, $J = 16.2$ Hz, H7). UV-visible (acetone): $\lambda_{max} = 339$ nm. IR (KBr): $\nu_{N=O} = 1342$ cm^{-1}. HRMS (FAB): calc. for $C_{26}H_{18}N_4O_2$ $[M + H]^+$ 450.1328; found 450.1339.

4,4′-Diformyl-[2,2′]-bipyridine (5). In a Schlenk flask, 4,4′-bis(*N*,*N*-dimethylaminovinyl)-[2,2′]-bipyridine **6** (1.7 g, 5.8 mmol, 1 equiv.) was dissolved in THF (180 mL) and an aqueous solution of $NaIO_4$ (10 g, 46.7 mmol, 8 equiv.) was added dropwise; the orange mixture turned white when stirred at 40 °C for 18 h. After cooling to room temperature, the solvent was removed under vacuum. The product was dissolved in dichloromethane (40 mL) and washed with water (2×50 mL). The organic phase was dried over $MgSO_4$, filtered, and the solvent then removed under vacuum. After precipitation from dichloromethane–pentane, **5** was finally obtained as a pale-yellow microcrystalline powder (1.45 g, 80% yield). ^{1}H NMR ($CDCl_3$): δ 10.19 (s, 2H, CHO), 8.92 (d, $J = 5$ Hz, 2H, H6), 8.85 (d, $^4J = 1.5$ Hz, 2H, H3), 7.75 (dd, $^3J = 5$ Hz, $^4J = 1.5$ Hz, 2H, H5). ^{13}C NMR ($CDCl_3$): δ 157.4 (C2), 157.0 (CHO), 150.7 (C6), 142.8 (C4), 121.7 (C5), 121.0 (C3). Mp = 192 °C. IR (KBr) $\nu_{C=O} = 1704$ cm^{-1}.

4,4′-Bis(*N*,*N*-dimethylaminovinyl)-[2,2′]-bipyridine (6). To a solution of 4,4′-dimethyl-[2,2′]-bipyridine (1.57 g, 8.5 mmol, 1 equiv.) in DMF (15 mL) was added under argon the Bredereck reagent [*tert*-butoxybis(diethylamino)methane; (8.1 mL, 39.1 mmol, 4.6 equiv.]. The mixture was then heated at 140 °C for 18 h. After cooling to room temperature, the pale orange mixture was hydrolyzed by addition of water (30 mL) and extracted with dichloromethane (4×30 mL). The organic phase was dried over $MgSO_4$ and the solvent removed under vacuum. The resulting orange solid was recrystallized from dichloromethane–pentane to give **6** as a saffron-yellow powder (2.4 g, 95% yield). ^{1}H NMR ($CDCl_3$): δ 8.30 (d, $J = 5.2$ Hz, 2H, H6), 8.10 (d, $^4J = 1.8$ Hz, 2H, H3), 7.15 (d, $J = 13.6$ Hz, 2H, H8), 6.91 (dd, $^3J = 5.2$ Hz, $^4J = 1.8$ Hz, 2H, H5), 5.02 (d, $J = 13.6$ Hz, 2H, H7), 2.83 (s, 12H, CH_3). ^{13}C NMR ($CDCl_3$): δ 156.2 (C2), 148.8 (C6), 148.7 (C4), 143.4 (C8), 118.0 (C5), 114.7 (C3), 94.5 (C7), 40.6 (C9). HRMS (FAB): calc. for $C_{18}H_{22}N_4$ $[M + H]^+$ 294.1844; found 294.1862.

4.4′-Bis(dibutylaminothienylvinyl)-[2,2′]-bipyridine (7). To a THF solution (20 mL) of diisopropylamine (1 mL, 7 mmol) at -20 °C was added ^{n}BuLi (1.6 M in hexane, 5 mL, 6.5 mmol) *via* syringe. The solution was then stirred for 15 min and a solution of 4,4′-dimethyl-[2,2′]-bipyridine (0.58 g, 3.1 mmol) in THF (30 mL) was added dropwise at -20 °C. The red mixture was stirred for 2 h. A solution of 5-(*N*,*N*-dibutylaminothiophene-2-carbaldehyde (1.5 g, 6.2 mmol) in THF (20 mL) was slowly added at -20 °C. The resulting yellow–green solution was stirred for 2 h at -20 °C and then at room temperature overnight. After hydrolysis and extraction with dichloromethane, the organic layers were dried over $MgSO_4$, filtered and the solvent was removed

under vacuum. The resulting yellow oil was dissolved in toluene (150 mL). After addition of a catalytic amount of pyridinium *p*-toluenesulfonate salt (0.1 g, 0.4 mmol), the red mixture was stirred under reflux for 4 h in a Dean–Stark apparatus. After evaporation of the toluene *in vacuo*, the residue was dissolved in dichloromethane and washed with a saturated aqueous solution of $NaHCO_3$. The organic layer was dried over $MgSO_4$, filtered and the solvent removed. After recrystallisation in ethyl acetate, compound **7** was obtained as a dark-red microcrystalline powder (1.77 g, 91%). ^{1}H NMR (CD_2Cl_2): δ 8.43 (d, $J=5.2$ Hz, 2H, H6), 8.33 (br s, 2H, H3), 7.39 (d, $J=15.8$ Hz, 2H, H8), 7.16 (dd, $^3J=5.2$ Hz, $^4J=1.6$ Hz, 2H, H5), 6.79 (d, $J=4$ Hz, 2H, H10), 6.35 (d, $J=15.8$ Hz, 2H, H7), 5.65 (d, $J=4$ Hz, 2H, H11), 3.21 (t, 8H, $J=7.5$ Hz, H13), 1.57 (m, 8H, H14), 1.30 (m, 8H, H15), 0.90 (t, 12H, H16). ^{13}C NMR (CD_2Cl_2): δ 158.95 (C12), 156.32 (C2), 149.22 (C6), 146.55 (C4), 130.94 (C10), 127.45 (C8), 124.06 (C9), 119.75 (C5), 117.95 (C7), 116.77 (C3), 100.68 (C11), 53.26 (C13), 29.22 (C14), 20.28 (C15), 13.74 (C16). HRMS (FAB): calc. for $C_{38}H_{50}N_4S_2$ $[M+H]^+$ 627.3555; found 627.3556.

4,4′-Bis(diethylaminophenylimino)-[2,2′]-bipyridine (8). 4,4′-Diformyl-[2,2′]-bipyridine (70 mg, 0.33 mmol) was dissolved in 10 mL of dichloromethane. *N*,*N*-Diethyl-1,4-phenylenediamine (0.12 mL, 0.69 mmol) and anhydrous magnesium sulfate (1 g) were added and the mixture was stirred for 2 h. The reaction mixture was filtered, the solvent evaporated, the resulting solid dissolved in dichloromethane and purified by precipitation with pentane to yield **8** as a yellow powder (0.24 g, 95%). Single crystals suitable for X-ray diffraction analysis were obtained by slow evaporation of a dichloromethane solution. ^{1}H NMR (CD_2Cl_2): δ 8.78 (br s, 2H, H3), 8.74 (d, $J=5.0$ Hz, 2H, H6), 8.61 (s, 2H, H7), 7.79 (dd, $^3J=5.0$ Hz, $^4J=1.5$ Hz, 2H, H5), 7.33 (d, $J=9.0$ Hz, 4H, H10), 6.69 (d, $J=9.0$ Hz, 4H, H11), 3.38 (q, $J=7.0$ Hz, 8H, H13), 1.16 (t, $J=7.0$ Hz, 12H, H14). ^{13}C NMR (CD_2Cl_2): δ 157.0 (C2), 151.7 (C7), 150.1 (C6), 148.2 (C12), 145.5 (C4), 138.5 (C9), 123.7 (C11), 121.7 (C5), 120.1 (C3), 112.1 (C10), 44.9 (C13), 12.8 (C16). HRMS (FAB): calc. for $C_{32}H_{37}N_6$ $[M+H]^+$ 505.3079; found 505.3088.

4,4′-Bis(dibutylaminophenylazo)-[2,2′]-bipyridine (9). 4,4′-Diamino-[2,2′]-bipyridine (0.5 g, 2.6 mmol) was dissolved in 10 mL of sulfuric acid (4 N) under argon. The solution was cooled to 0 °C and sodium nitrite (0.38 g, 5.5 mmol), dissolved in the minimum amount of water, was added with the temperature kept between 0 and 5 °C. After 30 min of stirring, *N*,*N*-dibutylaniline (1.25 g, 5.5 mmol) in THF (10 mL) was added dropwise to the diazonium salt solution. The solution was then allowed to warm to room temperature and the excess acid was neutralized by an aqueous solution of potassium hydroxide (4 N). The reaction mixture was filtered and extracted with dichloromethane. The organic layer was dried over magnesium sulfate and concentrated under reduced pressure. The crude product was then purified by silica gel column chromatography (dichloromethane–ether 1:1) to yield **9** as a dark-red solid (0.25 g, 25%). Orange crystals suitable for an X-ray diffraction study were obtained by slow evaporation of a dichloromethane-d^2 solution in an NMR tube. ^{1}H NMR (CD_2Cl_2): δ 8.76 (dd, 2H, $^3J=5.2$ Hz, $^5J=0.6$ Hz, H6), 8.71 (dd, 2H, $^4J=2.0$ Hz, $^5J=0.6$ Hz, H3), 7.88 (d, 4H, $J=9.2$ Hz, H11), 7.63 (dd, 2H, $^3J=5.2$ Hz, $^4J=2.0$ Hz, H5), 6.71 (d, 4H, $J=9.2$ Hz, H10), 3.38 (t, 8H, $J=7.6$ Hz, H13), 1.5 (m, 8H, H14), 1.30 (m, 8H, H15), 0.96 (t, 12H, $J=7.2$ Hz, H16). ^{13}C NMR (CD_2Cl_2): δ 159.3 (C4), 157.7 (C2), 151.8 (C12), 150.4 (C6), 143.0 (C9), 126.2 (C11), 116.2 (C5), 113.2 (C3), 111.2 (C10), 51.0 (C13), 29.4 (C14), 20.3 (C15), 13.7 (C16). HRMS (FAB): calc. for $C_{38}H_{51}N_8$ $[M+H]^+$ 619.4237; found 619.4255.

4,4′-Diamino-[2,2′]-bipyridine (10). In a typical experiment, 4,4′-dinitro-[2,2′]-bipyridine-[1,1′]-dioxide (3 g, 10.8 mmol) was dissolved in ethanol (100 mL) and 10% palladium on carbon was added (0.7 g). A solution of hydrazine monohydrate (2.5 mL, 54 mmol) in ethanol (20 mL) was added dropwise over a period of 1 h and the reaction mixture was refluxed for 8 h. The mixture was then filtered hot and washed with cold diethyl ether. The filtrate was evaporated under vacuum and the residue recrystallized from ethanol to yield **10** (2.01 g, 100%) as a yellow solid. ^{1}H NMR (DMSO-d^6): δ 7.89 (d, 2H, $J=5.5$ Hz, H6), 7.45 (d, 2H, $J=2.2$ Hz, H3), 6.42 (dd, 2H, $J=5.5$, $^4J=2.2$ Hz, H5), 5.92 (s, 4H, NH_2).

Typical procedure for successive additions of *p*-toluenesulfonic acid to 1. In a Schlenk flask, 4,4′-bis(dibutylaminostyryl)-[2,2′]-bipyridine (36 mg, 58.6 μmol) was dissolved in dichloromethane (100 mL) at room temperature. *p*-Toluenesulfonic acid (PTSA) was added, 1 equiv. at a time (1 equiv. = 11.2 mg, 58.6 μmol) and the mixture was stirred for 3 h, due to the low solubility of PTSA in CH_2Cl_2. A 1 mL aliquot was diluted in order to follow the reaction by UV-visible and fluorescence spectroscopy. The initially yellow solution turned deep-red after addition of 1 and 2 equiv. of PTSA. After further addition of acid (4 equiv.), the mixture became colorless.

[4,4′-Bis(dibutylaminostyryl)-[2,2′]-bipyridine][tetra-chloro-1,2-benzenediol]. In a Schlenk flask, 4,4′-bis(dibutylamino styryl)-[2,2′]-bipyridine (100 mg, 0.163 mol) and tetrachloro-1,2-benzenediol (40 mg, 0.163 mmol) were dissolved in dichloromethane (30 mL) at room temperature. The solution immediately turned yellow–brown. After 1 h of stirring, the solvent was evaporated and the product precipitated from dichloromethane–pentane to yield the title product as a brown powder (0.14 g, 100%). ^{1}H NMR (CD_2Cl_2): δ 8.30 (d, $J=4.5$ Hz, 2H, H6), 8.04 (br s, 2H, H3), 7.5 (br s, 2H, OH), 7.31 (d, $J=8.5$ Hz, 4H, H10), 7.20 (d, $J=16$ Hz, 2H, H8), 7.12 (masked, 2H, H5), 6.72 (d, $J=16.2$ Hz, 2H, H7), 6.58 (d, $J=8.5$ Hz, 4H, H11), 3.25 (t, $J=7$ Hz, 8H, H13), 1.5 (m, 8H, H14), 1.30 (m, 8H, H15), 0.92 (t, $J=7.2$ Hz, 12H, H16). ^{13}C NMR (CD_2Cl_2): δ 154.98 (C2), 148.62 (C12), 148.60 (C6), 147.75 (C4), 134.53 (C8), 129.71 (C10), 122.79 (C9), 120.42 (C5), 119.69 (C7), 118.21 (C3), 111.49 (C11), 50.70 (C13), 29.41 (C14), 20.30 (C15), 13.79 (C16), 144.32, 128.15, 121.90 [$Cl_4C_6(OH)_2$]. UV-visible (CH_2Cl_2): $\lambda_{max}=414$ nm. Anal. calc. (found) for $C_{48}H_{56}N_4Cl_4O_2\cdot 0.5CH_2Cl_2$: C 64.35 (63.83), H 6.35 (6.41), N 6.19 (5.96%).

Typical procedure for the complexation of 1. In a Schlenk flask, 4,4′-bis(dibutylaminostyryl)-[2,2′]-bipyridine (**1**) and the corresponding metallic salt [$HgCl_2$, $ZnCl_2$, $Zn(OAc)_2$, $PdCl_2$, Re_2O_7] were dissolved in dichloromethane (10 mL) at room temperature. The yellow solution turned from orange to deep violet depending on the nature of the metallic moiety. The solution was then concentrated *in vacuo* and microcrystalline product obtained from dichloro-methane–pentane.

(1)$HgCl_2$ (1a). Orange microcrystalline powder (80% yield). ^{1}H NMR (CD_2Cl_2): δ 8.19 (d, $J=5.5$ Hz, 2H, H6), 8.11 (br s, 2H, H3), 7.48 (d, $J=15.8$ Hz, 2H, H8), 7.48 (d, $J=9$ Hz, 4H, H10), 7.26 (d, $J=5.5$ Hz, 2H, H5), 6.76 (d, $J=15.8$ Hz, 2H, H7), 6.65 (d, $J=9$ Hz, 4H, H11), 3.31 (t, $J=7.4$ Hz, 8H, H13), 1.56 (m, 8H, H14), 1.36 (m, 8H, H15), 0.96 (t, $J=7.2$ Hz, 12H, H16). ^{13}C NMR (CD_2Cl_2): δ 150.07 (C2), 149.46 (C12), 148.76 (C4), 148.76 (C6), 137.31 (C8), 129.43 (C10), 122.31 (C9), 122.06 (C5), 118.54 (C3), 117.93 (C7), 111.50 (C11), 50.74 (C13), 29.43 (C14), 20.30 (C15), 13.79 (C16). Anal. calc. (found) for $C_{42}H_{54}N_4Cl_2Hg\cdot H_2O$: C 55.78 (55.64), H 6.24 (5.87), N 6.19 (6.30%).

*(1)$ZnCl_2$ (**1b**).* Orange microcrystalline powder (65% yield). ^{1}H NMR (CD_2Cl_2): δ 8.20 (d, $J=5.5$ Hz, 2H, H6), 8.11 (br s, 2H, H3), 7.60 (d, $J=16$ Hz, 2H, H8), 7.53 (d, $J=9$ Hz, 4H, H10), 7.18 (d, $J=5.5$ Hz, 2H, H5), 6.70 (d, $J=16$ Hz, 2H, H7), 6.67 (d, $J=9$ Hz, 4H, H11), 3.33 (t, $J=7$Hz, 8H, H13), 1.60 (m, 8H, H14), 1.40 (m, 8H, H15), 0.97 (t, $J=7.2$ Hz, 12H, H16). ^{13}C NMR (CD_2Cl_2): δ 150.95 (C2), 149.56 (C12), 148.34 (C4), 147.45 (C6), 138.38 (C8), 129.68 (C10), 122.19 (C9), 122.50 (C5), 116.80 (C3), 117.25 (C7), 111.42 (C11), 50.72 (C13), 29.39 (C14), 20.27 (C15), 13.79 (C16). Anal. calc. (found) for $C_{42}H_{54}N_4Cl_2Zn\cdot H_2O$: C 65.77 (65.75), H 7.36 (7.00), N 7.31 (7.40%).

*(1)$Zn(OCOCH_3)_2$ (**1c**).* Orange microcrystalline powder (65% yield). ^{1}H NMR (CD_2Cl_2): δ 8.51 (d, $J=5.5$ Hz, 2H, H6), 8.05 (br s, 2H, H3), 7.38 (d, $J=16$ Hz, 2H, H8), 7.44 (d, $J=9$ Hz, 4H, H10), 7.30 (d, $J=5.5$ Hz, 2H, H5), 6.73 (d, $J=16$ Hz, 2H, H7), 6.64 (d, $J=9$ Hz, 4H, H11), 3.30 (t, $J=7$Hz, 8H, H13), 1.58 (m, 8H, H14), 1.35 (m, 8H, H15), 0.95 (t, $J=7.2$ Hz, 12H, H16), 1.99 (s, 6H, $OCOCH_3$). ^{13}C NMR (CD_2Cl_2): δ 150.48 (C2), 149.37 (C12), 149.24 (C4), 148.82 (C6), 137.08 (C8), 129.26 (C10), 122.33 (C9), 121.89 (C5), 118.28 (C7), 117.31 (C3), 111.47 (C11), 50.70 (C13), 29.40 (C14), 20.29 (C15), 13.79 (C16), 179.80, 21.95 ($OCOCH_3$). Anal. calc. (found) for $C_{42}H_{54}N_4Cl_2Zn\cdot H_2O$: C 67.68 (67.84), H 7.65 (7.48), N 6.86 (7.01%).

*(1)$PdCl_2$ (**1d**).* Red–orange microcrystalline powder (90% yield). ^{1}H NMR (CD_2Cl_2): δ 8.93 (d, $J=6.2$ Hz, 2H, H6), 7.96 (br s, 2H, H3), 7.46 (d, $J=16$ Hz, 2H, H8), 7.46 (d, $J=8.9$ Hz, 4H, H10), 7.34 (dd, $^3J=6.2$ Hz, $^4J=1.5$ Hz, 2H, H5), 6.84 (d, $J=16$ Hz, 2H, H7), 6.63 (d, $J=8.9$ Hz, 4H, H11), 3.30 (t, $J=7.5$ Hz, 8H, H13), 1.56 (m, 8H, H14), 1.34 (m, 8H, H15), 0.94 (tr, $J=7.2$ Hz, 12H, H16). ^{13}C NMR (CD_2Cl_2): δ 156.21 (C2), 149.89 (C12), 149.76 (C4), 149.60 (C6), 138.28 (C8), 129.64 (C10), 121.99 (C9), 121.45 (C5), 118.40 (C3), 117.33 (C7), 111.52 (C11), 50.74 (C13), 29.40 (C14), 20.28 (C15), 13.76 (C16). Anal. calc. (found) for $C_{42}H_{54}N_4Cl_2Pd\cdot H_2O$: C 62.26 (62.19), H 6.97 (6.78), N 6.91 (7.34%).

*(1)$Re(CO)_3Cl$ (**1e**).* $Re(CO)_5Cl$ (88 mg, 24 μmol) and **1** (150 mg, 24 μmol, 1 equiv.) were stirred overnight in refluxing toluene (5 mL). The red solution was concentrated and the complex was precipitated upon addition of pentane (20 mL). After recrystallization from dichoromethane–pentane **1e** was obtained as a red microcrystalline powder (130 mg, 57%). ^{1}H NMR (CD_2Cl_2): δ (d, $J=5.9$ Hz, 2H, H6), 8.05 (br s, 2H, H3), 7.56 (d, $J=8.8$ Hz, 4H, H10), 7.29 (d, $J=16.3$ Hz, 2H, H8), 6.79 (d, $J=5.9$ Hz, 2H, H5), 6.69 (d, $J=8.8$ Hz, 4H, H11), 6.52 (d, $J=16.3$ Hz, 2H, H7), 3.31 (t, $J=7.7$ Hz, 8H, H13), 1.58 (m, 8H, H14), 1.3 (m, 8H, H15), 0.94 (t, $J=7.2$ Hz, 12H, H16). ^{13}C NMR (CD_2Cl_2 53.45): δ 198.3 (CO equatorial), 191.0 (CO axial), 155.7 (C2), 151.5 (C6), 149.5 (C12), 149.0 (C4), 137.8 (C8), 129.8 (C10), 123.0 (C5), 122.5 (C9), 118.8 (C3), 117.3 (C7), 111.7 (C11), 50.8 (C13), 29.4 (C14), 20.3 (C15), 13.8 (C16). Anal. calc. (found) for $C_{45}H_{54}N_4O_3ClRe$: C 58.71 (58.25), H 5.91 (5.79), N 6.09 (5.95%).

*[(1)$ReO_3]_2$-μ^2-O (**1f**).* Deep purple microcrystalline powder. (80% yield). ^{1}H NMR (CD_2Cl_2): δ 8.28 (d, $J=5.6$ Hz, 2H, H6), 8.23 (br s, 2H, H3), 7.36 (d, $J=8.8$ Hz, 4H, H10), 7.37 (d, $J=16$ Hz, 2H, H8), 7.22 (d, $J=5.6$ Hz, 2H, H5), 6.64 (d, $J=16$ Hz, 2H, H7), 6.54 (d, $J=8.8$ Hz, 4H, H11), 3.2 (t, $J=6.7$ Hz, 8H, H13), 1.5 (m, 8H, H14), 1.2 (br m, 8H, H15), 0.90 (t, $J=7.2$ Hz, 12H, H16).^{13}C NMR (CD_2Cl_2): δ 151.72 (C4), 149.62 (C12), 147.10 (C2), 144.95 (C6), 138.69 (C8), 129.98 (C10), 122.32 (C9), 121.14 (C5), 118.32 (C3), 117.77 (C7), 111.48 (C11), 50.74 (C13), 29.39 (C14), 20.26 (C15), 13.76 (C16). IR (KBr): $\nu_{(Re=O)}=911.5$ (vs), 967 (w) cm^{-1}. Anal. calc. (found) for $C_{84}H_{108}N_8O_7Re_2\cdot CH_2Cl_2$: C 56.74 (57.20), H 6.16 (6.46), N 6.41 (6.23%).

Acknowledgements

The authors would like to thank the Region Bretagne and France Telecom CNET for financial support. We gratefully acknowledge Brigitte Corre and Thomas Le Bouder for technical support.

References and notes

1 (*a*) *Molecular Nonlinear Optics, Materials, Physics and Devices*, ed. J. Zyss, Academic Press, New York, 1994; (*b*) D. M. Burland, *Chem. Rev.*, 1994, **94**, 1.
2 (*a*) J. L. Segura and N. Martin, *J. Mater. Chem.*, 2000, **10**, 2403; (*b*) R. E. Martin, F. Diederich and F. Hide, *Angew. Chem., Int. Ed.*, 1999, **38**, 1350; (*c*) A. Kraft, A. C. Grimsdale and A. B. Holmes, *Angew. Chem., Int. Ed.*, 1998, **37**, 403; (*d*) M. A. Diaz-Garcia, B. J. Schwartz and A. J. Heeger, *Acc. Chem. Res.*, 1997, **30**, 430.
3 (*a*) H. Ma, B. Chen, T. Sassa, L. R. Dalton and A. K.-Y. Jen, *J. Am. Chem. Soc.*, 2001, **123**, 986; (*b*) Y. Q. Shi, C. Zhang, H. Zang, J. H. Bechtel, L. R. Dalton, B. H. Robinson and W. H. Steier, *Science*, 2000, **288**, 119; (*c*) T. J. Marks and M. A. Ratner, *Angew. Chem., Int. Ed. Engl.*, 1995, **34**, 155.
4 J. L. Brédas, *Science.*, 1994, **263**, 487.
5 (*a*) S. R. Marder, D. N. Beratan and L. T. Cheng, *Science*, 1991, **252**, 103; (*b*) J. Roncali, *Chem. Rev.*, 1997, **97**, 173.
6 H. Le Bozec and T. Renouard, *Eur. J. Inorg. Chem.*, 2000, 229.
7 (*a*) A. Hilton, T. Renouard, O. Maury, H. Le Bozec, I. Ledoux and J. Zyss, *Chem. Commun.*, 1999, 2521; (*b*) M. Bourgault, K. Baum, H. Le Bozec, G. Pucetti, I. Ledoux and J. Zyss, *New J. Chem.*, 1998, **22**, 517.
8 (*a*) C. Dhenaut, I. Ledoux, I. D. W. Samuel, J. Zyss, M. Bourgault and H. Le Bozec, *Nature (London)*, 1995, **374**, 339; (*b*) H. Le Bozec, T. Renouard, M. Bourgault, C. Dhenaut, S. Brasselet, I. Ledoux and J. Zyss, *Synth. Met.*, 2001 in press.
9 T. Renouard, H. Le Bozec, I. Ledoux and J. Zyss, *Chem. Commun.*, 1999, 871.
10 (*a*) R. Ziessel, A. Juris and M. Venturi, *Inorg. Chem.*, 1998, **37**, 5061; (*b*) N. Armaroli, L. De Cola, V. Balzani, J.-P. Sauvage, C. O. Dietrich-Buchecker, J.-M. Kern and A. Bailal, *J. Chem., Soc., Dalton Trans.*, 1993, 3241.
11 H. S. Joshi, R. Jamshidi and Y. Tor, *Angew. Chem., Int. Ed.*, 1999, **38**, 2722.
12 A.-J. Attias, P. Hapiot, V. Witgens and P. Valat, *Chem. Mater.*, 2000, **12**, 461.
13 (*a*) A. Juris, S. Campagna, I. Bidd, J.-M. Lehn and R. Ziessel, *Inorg. Chem.*, 1988, **27**, 4007; (*b*) M. Bourgault, T. Renouard, B. Lognoné, C. Mountassir and H. Le Bozec, *Can. J. Chem.*, 1997, **75**, 318.
14 A.-J. Attias, C. Cavally, B. Bloch, N. Guillou and C. Noël, *Chem. Mater.*, 1999, **11**, 2057.
15 For a preliminary communication see: P. Dupau, T. Renouard and H. Le Bozec, *Tetrahedron Lett.*, 1996, **37**, 7503.
16 (*a*) O. Kocian, R. J. Mortimer and P. D. Beer, *Tetrahedron Lett.*, 1990, **31**, 5069; (*b*) M. Harding, U. Koert, J.-M. Lehn, A. Marquis-Rigault, C. Piguet and J. Siegel, *Helv. Chim. Acta*, 1992, **74**, 594.
17 M. G. Vetelino and J. W. Coe, *Tetrahedron Lett.*, 1994, **35**, 219.
18 (*a*) For an analogous phosphonate synthesis see: S. Nijhuis, G. L. A. Rikken, E. E. Havinga, W. Ten Hoeve, H. Wynberg and E. W. Meijer, *J. Chem. Soc., Chem. Commun.*, 1990, 1093; (*b*) A. Ulman, C. S. Willand, W. Köhler, D. R. Robello, D. J. Williams and L. Handley, *J. Am. Chem. Soc.*, 1990, **112**, 7083.
19 D. Prim, G. Kirsch and J.-F. Nicoud, *Synth. Lett.*, 1998, 383.
20 In the case of **2**, acidic impurities in deuterated chloroform are able to promote the isomerization of the double bond. Such phenomena are not observed in deuterated dichloromethane.
21 For analogous synthetic procedures of imino-containing dyes see: S.-S. Chou, D.-J. Sun, H.-C. Lin and P.-K. Yang, *Chem. Commun.*, 1996, 1045.
22 (*a*) I. R. Whittall, M. G. Humphrey, A. Persoons and S. Houbrechts, *Organometallics*, 1996, **15**, 1935; (*b*) I. R. Whittall, M. G. Humphrey, S. Houbrechts, A. Persoons and D. C. Hockless, *Organometallics*, 1996, **15**, 5738.
23 C. Colas and M. Goelner, *Eur. J. Org. Chem.*, 1999, 1357.
24 P. Wehman, G. C. Dol, E. R. Morrman, P. C. J. Kramer, P. W. N. M. V an Leeuwen, J. Fraanje and K. Goubitz, *Organometallics*, 1994, **13**, 4856.
25 H. Camren, M.-Y. Chang, L. Zen and E. McGuire, *Synth. Commun.*, 1996, **26**, 1247.

26 G. Maerker and F. H. Case, *J. Am. Chem. Soc.*, 1958, **80**, 2745.
27 For other molecular structures of 2,2′-bipyridines see: (*a*) M. H. Chisholm, J. C. Huffman, I. P. Rothwell, P. G. Bradley, N. Kress and W. H. Woodruff, *J. Am. Chem. Soc.*, 1981, **103**, 4945; (*b*) I. R. Butler and C. Soucy-Breau, *Can. J. Chem.*, 1991, **69**, 1117; (*c*) C. Bolm, M. Ewald, M. Zehnder and M. A. Neuburger, *Chem. Ber.*, 1992, **125**, 453.
28 C. Reichardt, *Chem. Rev.*, 1994, **94**, 2319.
29 The alkyl group of the $-NR_2$ moieties can be a methyl, an ethyl or a butyl. This slight modification has a small influence on the molecular extinction coefficient (Bu > Et > Me), but not on the λ_{max} position.
30 (*a*) L.-T. Cheng, W. Tam, S. R. Marder, A. E. Stiegman, G. Rikken and C. W. Spangler, *J. Phys. Chem.*, 1991, **95**, 10643; (*b*) M. Blanchard-Desce, V. Alain, P. V. Bedworth, S. R. Marder, A. Fort, C. Runser, M. Barzoukas, S. Lebus and R. Wortmann, *Chem. Eur. J.*, 1997, **3**, 1091; (*c*) V. Alain, M. Blanchard-Desce, I. Ledoux-Rak and J. Zyss, *Chem. Commun.*, 2000, 353.
31 A small positive solvatochromism of the absorption and emission bands is also observed for **7** (Fig. 5).
32 (*a*) V. P. Rao, A.-K. Jen, K. Y. Wong and K. J. Drost, *Tetrahedron Lett.*, 1993, **34**, 1747; (*b*) A.-K. Jen, V. P. Rao, K. Y. Wong and K. J. Drost, *J. Chem. Soc., Chem. Commun.*, 1993, 90; (*c*) A.-K. Jen, Y. Cai, P. V. Bedworth and S. R. Marder, *Adv. Mater., 1997,* **9**, 132; (*d*) V. P. Rao, A.-K. Jen, K. Y. Wong and K. J. Drost, *J. Chem. Soc., Chem. Commun.*, 1993, 1118; (*e*) X. Wu, J. Wu, Y. Liu and A.-K. Jen, *J. Am. Chem. Soc.*, 1999, **121**, 472; (*f*) V. P. Rao, A. K.-Y. Jen and Y. Cai, *Chem. Commun.*, 1996, 1237.
33 T. L. Gilchrist, *Heterocycle Chemistry*, J. Wiley Sons Inc., New York, 1985.
34 For some theoritical aspects see: (*a*) I. D. L. Albert, T. J. Marks and M. A. Ratner, *J. Am. Chem. Soc.*, 1997, **119**, 6575; (*b*) E. M. Breitung, C.-F. Shu and R. J. McMahon, *J. Am. Chem. Soc.*, 2000, **122**, 1154 and references cited therein.
35 T. Tsunekawa and K. Yamaguchi, *J. Phys. Chem.*, 1992, **96**, 10 268.
36 (*a*) A. K.-J. Jen, X. Wu and H. Ma, *Chem. Mater.*, 1998, **10**, 471; (*b*) C.-F. Shu, Y.-C. Shu, Z.-H. Gong, S.-M. Peng, G. H. Lee and A. K.-J. Jen, *Chem. Mater.*, 1998, **10**, 3284; (*c*) Y.-C. Shu, Z.-H. Gong, C.-F. Shu, E. M. Breitung, R. J. McMahon, G. H. Lee and A. K.-J. Jen, *Chem. Mater.*, 1999, **11**, 1628; (*d*) X. Wu, J. Wu, Y. Liu and A. K.-J. Jen, *Chem. Commun.*, 1999, 2391; (*e*) J.-M. Raimundo, P. Blanchard, I. Ledoux-Rak, R. Hierle, L. Michaud and J. Roncali, *Chem. Commun.*, 2000, 1597.
37 The UV-visible spectrum of a dichloromethane solution of 2,2′-bipyridine in the presence of trifluoroacetic acid shows an absorption band at 311 nm.
38 (*a*) R. Andreu, I. Malfant, P. Lacroix, H. Gornitzka and K. Nakatani, *Chem. Mater.*, 1999, **11**, 840; (*b*) S. R. Marder, J. W. Perry and C. P. Yakymyshyn, *Chem. Mater.*, 1994, **6**, 1137.
39 M. Maus and K. Rurack, *New J. Chem.*, 2000, **24**, 677.
40 C. C. Evans, M. Bagieu-Beucher, R. Masse and J.-F. Nicoud, *Chem. Mater.*, 1998, **10**, 847.
41 (*a*) I. Majerz, Z. Malarski and L. Sobczyk, *Chem. Phys. Lett.*, 1997, **247**, 361; (*b*) S. Huang, D. Britton, M. C. Etter and S. R. Byrn, *J. Mater. Chem.*, 1997, **7**, 713.
42 T. Steiner, C. C. Wilson and I. Majerz, *Chem. Commun.*, 2000, 1231.
43 The UV-visible spectrum could not be recorded in classical dilute solution due to dissociation of the adduct upon dilution. The spectrum was recorded on a concentrated liquid film precluding the extinction coefficient measurement.
44 Formation of Zn(II) complexes with the alkoxy-containing ligand **2** is accompanied by a partial *E–Z* isomerization of the double bond: B. Lognoné and H. Le Bozec, unpublished results.
45 W. A. Herrmann, P. Kiprof, K. Rypdal, J. Tremmel, R. Blom, R. Alberto, J. Behm, R. W. Albach, H. Bock, B. Solouki, J. Mink, D. Lichtenbeger and N. E. Gruhn, *J. Am. Chem. Soc.*, 1991, **113**, 6527.
46 H. Arzoumanian, R. Bakhtchadjian, G. Agrifoglio, H. Krentzien and J.-C. Daran, *Eur. J. Inorg. Chem.*, 1999, 2255.
47 S. Kobayashi, T. Busujima and S. Nagayama, *Chem. Eur. J.*, 2000, **6**, 3491.
48 M. E. Huston, K. W. Haider and A. W. Czarnik, *J. Am. Chem. Soc.*, 1988, **110**, 4460.
49 (*a*) M. C. Kimber, I. B. Mahadevan, S. F. Lincoln, A. D. Ward and E. R. T. Tiekink, *J. Org. Chem.*, 2000, **65**, 8204 and references cited therein; (*b*) G. K. Walkup, S. C. Burdette, S. J. Lippard and R. Y. Tsien, *J. Am. Chem. Soc.*, 2000, **122**, 5644; (*c*) T. Hirano, K. Kikuchi, Y. Urano, T. Higuchi and T. Nagano, *J. Am. Chem. Soc.*, 2000, **122**, 12399.
50 J. N. Demas and G. A. Crosby, *J. Phys. Chem.*, 1971, **75**, 991.
51 C. K. Fair, MolEN, An Interactive Intelligent System for Crystal Structure Analysis, Enraf–Nonius, Delft, The Netherlands, 1990.
52 A. L. Spek, HELENA, Program for the Handling of CAD4-Diffractometer Output SHELX(S/L), Utrecht University, The Netherlands, 1997.
53 A. Altomare, M. C. Burla, M. Camalli, G. Carscarano, C. Giacovazzo, A. Guagliardi, A. G. G. Moliterni, G. Polidori and R. Spagna, *J. Appl. Crystallogr.*, 1998, **31**, 74.
54 G. M. Sheldrick, SHELX93, Program for the Refinement of Crystal Structures, University of Göttigen, Germany, 1993.
55 A. L. Spek, PLATON, A Multipurpose Crystallographic Tool, Utrecht University, The Netherlands, 1998.
56 T. Yoshida and S. Saito, *Bull. Chem. Soc. Jpn.*, 1982, **55**, 3047.
57 R. Brette, D. A. Dunmur, N. J. Hindeley and C. M. Marson, *J. Chem. Soc., Perkin Trans. 1*, 1993, 775.
58 Other sources of $NaIO_4$ used for the oxidation of **6** to **5** gave only poor yields.